Research article

How is the activity of shikimate dehydrogenase from the root of *Petroselinum crispum* (parsley) regulated and which side reactions are catalyzed?

Veronika Hýsková[a*], Kateřina Bělonožníková[a], Ingrida Šmeringaiová[a], Daniel Kavan[a], Marek Ingr[a,b] Helena Ryšlavá[a]

[a]*Department of Biochemistry, Faculty of Science, Charles University, Hlavova 2030, Prague 2, 128 40, Czech Republic*

[b]*Tomas Bata University in Zlín, Faculty of Technology, Department of Physics and Materials Engineering, Nám. T.G. Masaryka 5555, 760 01 Zlín, Czech Republic*

[*]Corresponding author at: Charles University, Hlavova 2030, Prague 2, 128 40, Czech Republic

E-mail addresses: veronika.hyskova@natur.cuni.cz (V. Hyskova) katerina.belonoznikova@natur.cuni.cz (K. Belonoznikova), smer.inga@gmail.com (I. Smeringaiova), daniel.kavan@natur.cuni.cz (D. Kavan), marek.ingr@natur.cuni.cz (M. Ingr), helena.ryslava@natur.cuni.cz (H. Ryslava)

Tel: +420 221 951 282; fax: +420 221 951 283

Graphical Abstract:

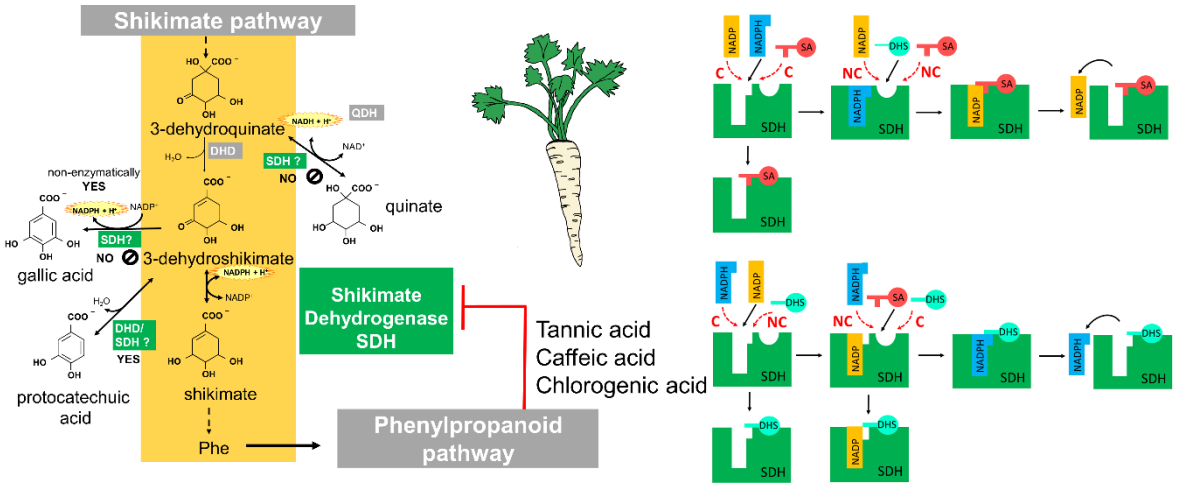

Highlights

- *Petroselinum crispum* (parsley) SDH follows an ordered reaction mechanism with three dead-end complexes.
- Gallic acid and quinate are not direct bypass products of parsley SDH.
- Tannic acid, chlorogenic acid, and caffeic acid effectively inhibit SDH.
- Parsley SDH also forms protocatechuic acid in an irreversible reaction.

Abstract

Inhibitors of the shikimate pathway are widely used as herbicides, antibiotics, and anti-infectious drugs. However, the regulation of the shikimic pathway is complex, and little is known about the feedback regulation of the shikimate dehydrogenase (SDH, EC 1.1.1.25) in plants. Thus, the aim of this study was to elucidate the kinetic mechanism of SDH purified from the root of *Petroselinum crispum* (parsley), to determine all possible reaction products and to identify phenylpropanoid compounds that affect its activity. Our results showed that the bisubstrate reaction catalyzed by *P. crispum* SDH follows a sequential ordered mechanism, except for three dead-end complexes. The main and lateral reactions of SDH were monitored by mass spectrometry, thereby detecting protocatechuic acid as a byproduct. Gallic acid was formed non-enzymatically, whereas quinate was not detected. Several polyphenolic compounds inhibited SDH activity, especially tannic, caffeic and chlorogenic acids, with IC_{50} 0.014 mM, 0.15 mM, and 0.19 mM, respectively. The number of hydroxyl groups influenced their inhibition effect on SDH, and *p*-coumaric, *t*-ferulic, sinapic, syringic and salicylic acids were less effective SDH inhibitors. Nevertheless, one branch of the phenylpropanoid pathway may affect SDH activity through feedback regulation.

Keywords: *Petroselinum crispum*; Apiaceae; chlorogenic acid; dehydroshikimate; gallic acid; hydroxycinnamic acids; simple phenols; tannic acid.

Abbreviations: AMP, 2-amino-2-methyl-1-propanol; DHD, 3-dehydroquinate dehydratase DHS, 3-dehydroshikimate; DHQ, 3-dehydroquinate; GA, gallic acid; PCA, protocatechuic acid; SA, shikimic acid; SDH, shikimate dehydrogenase; QA, quinate.

1. Introduction

The shikimate pathway is well known for the synthesis of aromatic amino acids in bacteria, fungi, apicomplexan parasites, and plants. In turn, this pathway is absent in animals. For this reason, inhibitors of individual enzymes were identified as antimicrobial agents and herbicides (Carrington et al., 2018; Deng and Lu, 2017; Tzin and Galili, 2010). The key enzyme of the shikimate pathway is shikimate dehydrogenase (SDH, EC 1.1.1.25). In plants, SDH is a bifunctional enzyme that catalyzes steps three and four. The N-terminal domain functions as 3-dehydroquinate dehydratase (DHD, EC 4.2.1.10), the C- terminal domain catalyzes the reduction of 3-dehydroshikimate (DHS) to shikimate (SA) in the presence of NADPH. The regulation of the shikimate pathway in plants is more complex than in bacteria and yeast (Carrington et al., 2018; Deng and Lu, 2017; Heldt et al., 2011; Tzin and Galili, 2010). The products of the shikimate pathway include not only phenylalanine, tyrosine, and tryptophan but also a wide range of polyphenolic compounds, such as phenolic acids, lignans, lignin, flavonoids, stilbenes and tannins. These compounds can protect plants against oxidative stress and UV radiation, impregnate cell walls and have antimicrobial properties. Thus, secondary metabolites are often synthetized and accumulated in plants in response to various stress conditions and can be associated with increased SDH activity (Belonoznikova et al., 2020; Cabane et al., 2004; Hyskova et al., 2017; Kovacik et al., 2009; Moura et al., 2010).

Another reaction catalyzed by SDH was proposed in walnut (*Juglans regia*) and *Escherichia coli*, in which 3-DHS was identified as the substrate of SDH in the presence of NADP. In the proposed SDH reaction mechanism, 3-DHS is oxidized to 3,5-didehydroshikimate, and gallic acid is formed after enolization, thereby continuously generating both shikimate and gallic acid (Muir et al., 2011). Therefore, this reaction is important for plants such as grapevine

(*Vitis vinifera*) that produce derivates of gallic acid, epicatechin 3-gallate and β-glucogallin, (Bontpart et al., 2016).

Guo *et al.* (2014) and Tahara *et al.* (2021) also described the synthesis of quinate (QA) from 3-dehydroquinate (DHQ) by DHD/SDH from poplar (*Populus trichocarpa*), and from *Eucalyptus camaldulensis*, respectively. However, only some members of the gene family catalyzed this reaction in which NADH is used for reduction instead of NADPH (Guo et al., 2014; Tahara et al., 2021). These reactions were described in plants with more than one gene for DHD/SDH, which could be separated into groups with "classical" SDH activity and groups that produce quinic acids (Bontpart et al., 2016; Guo et al., 2014; Muir et al., 2011). Moreover, another SDH side reaction – DHS dehydration to protocatechuic acid (PCA) – is also considered (Bontpart et al., 2016; Muir et al., 2011).

As with other enzymes of the shikimate and phenylpropanoid pathways, SDH is localized in chloroplasts where the reducing equivalents of NADPH and ATP from photosynthesis are available. On the other hand, in non-photosynthetic plastids, the reducing equivalents of NADPH required for synthetic pathways are provided by the oxidative pentose phosphate cycle, i.e., glucose-6-phosphate dehydrogenase and 6-phosphogluconate dehydrogenase (Esposito et al., 2003). Although the shikimate pathway is a very important metabolic flow in plants, the regulation of its key enzyme (SDH) by phenylpropanoid compounds and possible SDH products are less studied, especially in non-photosynthetic tissues.

Considering the above, this study aimed to find a plant source with naturally high SDH activity and to study the kinetic properties of SDH from non-photosynthetic tissue. Root tissue of *Petroselinum crispum* (Mill.) Fuss (Apiaceae) (parsley) was identified as suited to this purpose. The mechanism of reaction was characterized in both directions, thus gaining insights into dead end complexes involved in the regulation of SDH activity. The effect of

phenolic compounds as potential inhibitors was tested, and the results show that not only tannic acid but also caffeic acid and chlorogenic acid function as SDH strong inhibitors.

2. Results

2.1. Characterization of P. crispum root SDH: typical high pH optimum and 61.5 kDa molecular weight

SDH activity was screened in crude extracts from 8 different vegetables. Onion and broccoli crude extracts had low SDH activity, whereas crude extracts from *P. crispum* root and zucchini were identified as the richest sources of SDH among all plants tested. A high SDH activity per gram of fresh weight correlates with a low total phenolics content and *vice versa* (Fig.1). SDH was purified by ion exchange and gel chromatography from *P. crispum* (*Petroselinum crispum*) root to a final specific activity of 470 ± 18 $nmol.min^{-1}.mg^{-1}$.

SDH activity was pH-dependent, with a pH optimum between 7-8.5 and 9.5- 10 in the physiological and reverse reactions, respectively (Table 1). The molecular weight was 63 kDa when determined by red native electrophoresis (Fig. 2A) and 60 kDa when assessed by gel chromatography (Fig. 2B). The isoelectric point of *P. crispum* SDH was 4.5 (Fig. 2C). Only one protein band with SDH activity was detected after native red electrophoresis and isoelectric focusing. During gel chromatography, SDH was eluted as a single peak. Thus, only one isoform of SDH is present in *P. crispum* root.

2.2. The kinetic properties of P. crispum SDH differ from those of other dehydrogenases

The kinetic parameters of the reaction catalyzed by *P. crispum* root SDH were studied in both directions, i.e., in the physiological (shikimate pathway) direction: NADPH + DHS $\rightarrow$ SA + NADP, and in the reverse direction: SA + NADP $\rightarrow$ NADPH + DHS (Fig. 3). The Michaelis constants and maximal velocities are summarized in Table 1. The maximal reaction rate for the reverse reaction from SA to DHS was 4.6-fold higher than in the shikimate pathway direction (DHS reduction). Because the saturating concentrations of NADP and SA

were high, we also determined the apparent Michaelis constant at approximate conditions (Table 1). Furthermore, excess substrate DHS inhibited the reaction (Fig. A.1) with a substrate inhibition constant of K_{SS} = 0.12 ± 0.07 mM (Table 1).

2.3. Product inhibition analysis confirmed the ordered mechanism of the SDH-catalyzed reaction in both directions

The kinetic mechanism of the bisubstrate SDH reaction was analyzed in both directions. To identify the type of mechanism, we constructed Lineweaver-Burk diagnostical plots (Fig. 3), a Hanes plot and an Eadie-Hofstee plot (data not shown) and performed product inhibition assays (Fig. 4, Table 2). All kinetic parameters including V_{max}, K_m, K_A, K_{ic}, K_{iu}, K_i, $V^*_{max,}$ K_{SS}, $S_{0.5}$ were calculated from non-linear regression using Eqs. 1-7.

The initial rate of the reaction in the physiological direction was measured using several concentrations of DHS and NADPH, showing the typical Lineweaver-Burk plot of a sequential mechanism: straight lines with an intercept left to the ordinate (Fig. 3) and K_A 0.25 ± 0.13 mM. In this direction, the free enzyme binds to NADPH, which allows DHS, but not SA, binding in an ordered mechanism, thus partly explaining the mutual competition between NADPH and SA. NADPH binding apparently prevents NADP binding, and *vice versa*, leading to bilateral mutual competitive inhibition (Fig. 5, Table 2).

The direction of SA oxidation confirmed the strong affinity between the free enzyme and NADP. The mechanism was sequential but with a very low, almost immeasurable, dissociation constant for the complex enzyme – substrate (K_A), thus it seems to look like a ping-pong. Obviously, the complex enzyme-NADP is very thermodynamically stable (Fig. 3).

NADP binding enables both DHS and SA binding. The latter follows a classical ordered mechanism in the direction of SA + NADP → NADPH + DHS; in contrast, the former results in the formation of a dead-end complex. Its origin explains the competitive

inhibition of DHS against the substrate SA. Thus, these findings further confirm the competition between NADP and NADPH (Fig. 5, Table 2).

DHS binding to the free enzyme prevents NADPH binding by forming a dead-end complex (enzyme-DHS) that precludes a disordered mechanism in the direction of NADPH + DHS $\rightarrow$ SA + NADP. In addition, another dead-end complex (enzyme-DHS-NADP) is also formed when NADP binds to the enzyme-DHS (Fig. 5).

SA binding to the free enzyme prevents both NADP and NADPH binding also by forming a dead-end complex, which, in the case of NADP, prevents a disordered mechanism in the direction of SA + NADP $\rightarrow$ NADPH + DHS. In the case of NADPH, the formation of the dead-end complex completes the explanation for the competitive inhibition by the SA inhibitor against the NADPH substrate. Thus, SA competes with NADPH to bind to free enzyme, but not the other way around, that is, NADPH does not compete with SA since SA binding to the enzyme leads to a dead-end complex. Therefore, we proposed an ordered mechanism of the bi-substrate reaction catalyzed by SDH in both directions with three dead-end complexes (enzyme-DHS, enzyme-SA, and enzyme-NADP-DHS) (Fig. 5).

2.4. Identification of all SDH products and cofactor specificity

The activity of SDH was monitored by LC-MS (Table 3), focusing on side reactions. GA was formed non-enzymatically since it was also detected without SDH in the mixtures. PCA was produced from SA and DHS in the *P. crispum* shikimate pathway. No products were detected for DHQ with NADH and for QA with NAD as substrates. The *P. crispum* SDH active routes are shown in Fig. 6.

2.5. Tannic acid and some phenylpropanoids, as well as Zn^{2+} and Cu^{2+} ions, inhibit SDH activity

Various compounds that participate in phenylpropanoid metabolism and/or are related to SDH were studied as potential modulators of its activity in a screening performed at

inhibitor concentrations ranging from 0.006 to 3.5 mM. Aromatic amino acids (Phe, Tyr, Trp), which are synthesized in the shikimate pathway, had no effect on SDH activity. Concurrently, the first product of the phenylpropanoid pathway (*t*-cinnamic acid) and the potential SDH product (quinic acid) did not affect SDH activity, similarly to umbelliferone (7-hydroxycoumarine) and resveratrol (trans–3,4',5–trihydroxystilbene) (Fig. 7). One-way ANOVA confirmed that the effect of these compounds was non-significant (data not shown). In turn, salicylic, *p*-coumaric, *t*-ferulic, sinapic, syringic, caffeic, chlorogenic (caffeic acid and quinic acid ester) acids and the polyphenolic compound tannic acid had an inhibitory effect on *P. crispum* SDH activity, with tannic acid showing the lowest IC_{50} (Fig. 7). Caffeic acid and chlorogenic acid were also effective inhibitors. Hydroxycinnamic acids, such as *p*-coumaric, *t*-ferulic, sinapic, syringic and salicylic acids, showed much higher IC_{50} values (Fig. 7). In the irreversible inhibition test, the activity of the enzyme incubated with individual inhibitors did not decrease over time (data not shown). Therefore, all inhibitors mentioned above are reversible.

Although gallic acid was also tested, it strongly interfered with the formation of color complexes, making it impossible to determine its effect. Furthermore, the color of flavanone or any representative of the flavonoids interfered with the colorimetric method, also precluding the analysis of their inhibitory activity.

Table 4 summarizes the effects on SDH activity when adding different ions to the reaction mixture. Generally, among the ions tested in this study (Ca^{2+}, Na^{+}, K^{+}, Mg^{2+}, Mn^{2+}, Zn^{2+}, and Cu^{2+}), only Zn^{2+} and Cu^{2+} had a significant effect on SDH activity. At 0.1 mM and 0.01 mM, $Zn^{2+}$and Cu^{2+} decreased SDH activity to 10 and 21 %, respectively.

3. Discussion

The kinetic study of SDH purified from non-photosynthetic tissue *P. crispum* root containing evaluation of product inhibitors, Michaelis constants and pH optima of both reversible reactions resulted in establishing an ordered mechanism and shift of the equilibrium in favor of physiological shikimate pathway direction in the cell. Furthermore, *P. crispum* SDH exclusively used NADP(H) and SA (DHS) as a coenzyme and a substrate, respectively, while forming PCA as a by-product but not being involved in GA production. Furthermore, phenylpropanoids of one branch were found responsible for feedback regulation of *P. crispum* SDH.

3.1. P. crispum root extracts show high SDH activity

One of the reasons why SDH activity is low in plant crude extracts is the presence of phenolics. In general, when exposed to air, plant phenolics are readily oxidized, generating products that form complexes with proteins and inhibit enzyme activity (Buchanan et al., 2000), as shown in Fig. 1. Since the total phenolic content is very high in plants, especially in medicinal herbs (Tupec et al., 2017), a group of vegetables was chosen to identify a source of high SDH activity from non-photosynthetic tissue. From the group of 8 vegetable sources, the *P. crispum* root exhibited the highest SDH activity.

3.2. The directions of SDH-catalyzed SA oxidation and DHS reduction is controlled by the pH optimum and differ in maximal reaction rate

SDHs catalyze a reversible reaction, both DHS reduction and SA oxidation. For *P. crispum* SDH, the optimal pH was 9.5-10 for SA oxidation and 7-8.5 for DHS reduction (i.e., shikimate pathway direction) (Table 1). Accordingly, pH likely participates in the regulation of SDH activity *in vivo*. In photosynthetic tissues, the optimal pH 8 of the SDH reaction in the shikimate pathway direction matches the pH of the illuminated chloroplast, which ensures that the reactions of the shikimate pathway coincide with photosynthesis, and thus NADPH and

ATP are readily available. Although SDH purified from *P. crispum* root is not a chloroplastic enzyme, SDH regulation by pH in non-photosynthesizing plastids is likely similar. NADPH is provided by the oxidative pentose phosphate pathway, and the optimal pH of glucose-6-phosphate dehydrogenase from barley root plastids is also approximately pH 8 (Esposito et al., 2001). Conversely, SDHs have a non-physiologically high optimal pH in the SA oxidation direction (Avitia-Dominguez et al., 2014; Diaz and Merino, 1997; Guo et al., 2014; Lourenco and Neves, 1984; Lourenco et al., 1991). The unusually high optimal pH of the reverse reaction may be a mechanism of physiological protection against metabolite flowback through the shikimate pathway (Table 1). The pH profiles of SDH suggest that catalysis and substrate binding involve acid/base chemistry (Fonseca et al., 2007). The amino acids residues Lys385 and Asp423 (numbered with respect to the *Arabidopsis* protein), located in the SDH active site, which are conserved in DHD/SHD enzymes and which have been proposed to be involved in proton transfer during catalysis, are most likely responsible for such a high optimal pH (Singh and Christendat, 2006).

Furthermore, other factors favor the direction of shikimate pathway: metabolite channeling, which prevents the accumulation of substrates or products (Singh and Christendat, 2006), high Michaelis constants in the direction of SA oxidation (Table 1), product competitive inhibition against NADP and SA (Fig. 4, 5) and the formation of dead-end complexes (Fig. 5). The comparison of the maximal reaction rate in both directions shows that the reaction is 4.6 times higher in the non-physiological direction. These data were obtained at the pH optimum of the respective reactions, so they are not likely relevant to cellular context. However, this reaction is often used to study the properties of SDH from various sources.

For many SDHs, the bisubstrate reaction follows a typical sequential mechanism, as found for SDH from other sources, e. g., *Pisum sativum* (Balinsky et al., 1971; Dowsett et al., 1972) or *Capsicum annuum* (Diaz and Merino, 1997) or from *Mycobacterium tuberculosis* (Fonseca et

al., 2007). In pea epicotyls, the sequential mechanism of the bisubstrate reaction was further specified to be ordered, with NADPH binding followed by DHS (Balinsky et al., 1971; Dowsett et al., 1972). The mechanism of mycobacterial SDH was also classified as steady-state ordered, albeit with DHS binding first, followed by NADPH (Fonseca et al., 2007). Bacterial and plant SDHs also differ in their genetic framework in that each enzyme of the shikimate pathway is encoded by monofunctional genes in bacteria. In turn, DHD and SDH are fused to a bifunctional enzyme complex in plants, and even 5 enzymes of the shikimate pathway are fused to a penta-functional complex in fungi (Derrer et al., 2013). *P. crispum* SDH has the typical molecular weight of plant SDHs (Fig. 2) (Bontpart et al., 2016; Diaz and Merino, 1997; Fiedler and Schultz, 1985; Koshiba, 1978; Lourenco and Neves, 1984; Lourenco et al., 1991; Muir et al., 2011) and is likely a monomer with both domains, DHD and SDH. The initial reaction rate (Fig. 3) and product inhibition pattern (Fig. 4) are in line with an ordered bi-bi mechanism with NADPH or NADP binding to the enzyme first except that SA is a competitive inhibitor with respect to NADPH and DHS is a competitive product inhibitor with respect to SA (Fig. 5). These findings indicate that not only NADPH and NADP but also SA may interact with the free enzyme, most likely in the form of a dead-end complex (enzyme-SA). Both NADP and SA prevent the first substrate, NADPH, from binding to SDH, but DHS has no competitive inhibitor. Therefore, in accordance with an ordered mechanism, DHS is the second substrate. Nevertheless, the enzyme-DHS complex acts as a dead-end complex, similarly to enzyme-NADP-DHS (Fig. 5). Hence, the formation of dead-end complexes with SA and DHS explains the key role that the NADP/NADPH ratio plays in establishing an equilibrium between the two directions. In *P. crispum*, the shikimate pathway *via* NADPH continues with the phenylpropanoid pathway, specifically with the synthesis of coumarins, where psoralen, bergapten, isoimperatorin, oxypeucedanin, xanthoxin, trioxalen, and angelicin are the most important coumarins in *P. crispum*, or with the synthesis of

flavonoids (apiin and luteolin) (Kolarovic et al., 2010). In addition to the shikimate pathway, NADPH is also needed for the antioxidant system and for nitrate assimilation.

3.3. SDH also catalyzes the formation of PCA but not GA and QA

Other SDH-catalyzed reactions that may provide phenolic compounds or intermediates have been reported. Muir et al. (2011) demonstrated that SDH from walnut (*Juglans regia*) catalyzed not only the NADP-dependent dehydrogenation of SA to DHS but also the dehydrogenation of DHS to 3,5-diDHS, which provides GA after enolization. Recombinant EcDQD/SDH2 and 3 enzymes also catalyze NADP-dependent oxidation of 3-DHS to produce gallate, which is in some Eucalyptus species essential for the biosynthesis of the aluminum-detoxifying metabolite (Tahara et al., 2021). Two SDH isoforms showed a similar activity in grape wine berries (Bontpart et al., 2016). However, when analyzing *P. crispum* SDH, we also detected GA in the mixtures without the enzyme (Table 3). Therefore, we confirmed that GA could form non-enzymatically, as found in an *in vitro* study of recombinant isoforms of *Camellia sinensis* SDHs of grape wine berries (Huang et al., 2019) and also non-enzymatic formation of gallic acid was previously described (Kambourakis and Frost, 2000). Moreover, the reaction mechanism of *P. crispum* SDH showed that the binding of NADP and DHS to the SDH leads to the dead-end complex (Fig. 5). Consequently, enzymatic GA formation is not possible.

We also studied the pathway from DHQ to QA and back, but no products were detected in both directions. Thus, P. *crispum* SDH also belongs to the *bona fide* SDH group, using exclusively NADP as a coenzyme and SA as a substrate (Garcia-Guevara et al., 2017), whereas, e.g., some poplar and *Eucalyptus camaldulensis* SDH isoforms prefer NAD and also use QA as a substrate (Guo et al., 2014; Tahara et al., 2021). In-depth sequencing and *in vitro* biochemical assays showed that 3 poplar enzymes from 5 originally annotated as DHD/SDHs should be rather classified as QA dehydrogenases (Guo et al., 2014). In turn, we found that

PCA is a byproduct in the *P. crispum* SDH pathway (Table 3, Fig. 6). As previously hypothesized (Guo et al., 2014), this reaction is ensured by SDH in *P. crispum*.

3.4. P. crispum root SDH is regulated by metabolites of the phenylpropanoid pathway

Because the shikimate pathway is absent in mammals, searching and designing inhibitors against enzymes of this pathway may lead to the development of antimicrobials (such as the bacterial *Mycobacterium tuberculosis* and *Helicobacter pylori* SDH) and antiparasitic (malaria parasite SDH) and herbicidal (plant SDH) agents, which are harmless to humans (Diaz-Quiroz et al., 2018). There are 3 strategies for identifying compounds with an inhibitory effect on a particular enzyme: i) analyzing substrate structural analogs (Baillie et al., 1972; Diaz and Merino, 1997; Fiedler and Schultz, 1985; Koshiba, 1978; Lemos Silva et al., 1985; Lourenco and Neves, 1984; Lourenco et al., 1991; Rothe, 1974), ii) screening thousands of compounds (Avitia-Dominguez et al., 2014; Han et al., 2006; Peek et al., 2014), and iii) searching for feedback inhibitors among products of the whole pathway. The first strategy has led to the discovery of the herbicide 2,4-dichlorphenoxy acetic acid (2,4-D) (Diaz and Merino, 1997). Concurrently, several studies have demonstrated that PCA (possible byproduct of SDH) inhibits plant SDH (Diaz and Merino, 1997; Koshiba, 1978; Lemos Silva et al., 1985; Lourenco and Neves, 1984; Lourenco et al., 1991). In this study, we have shown that *P. crispum* SDH forms PCA in the irreversible reaction (Fig. 6). Using a screening strategy, different research groups have identified SDH inhibitors, for example, 5 novel *Helicobacter pylori* SDH inhibitors, including the natural product curcumin (Han et al., 2006), and polyphenolic inhibitors (epigallocatechin gallate and epicatechin gallate) of *Pseudomonas putida* and *Arabidopsis thaliana* SDH (Peek et al., 2014). A limited number of inhibition/activation studies have identified dihydroxybenzoic acid and its derivatives as SDH inhibitors (Fiedler and Schultz, 1985; Koshiba, 1978; Nandy and Ganguli, 1961), thus showing that SDH inhibitors are not limited to herbicides and organic reagents.

In this study, we chose the third strategy to identify plant SDH inhibitors among the products of the phenylpropanoid pathway (representative compounds of simple phenols, flavonoid, stilbene, and polyphenols). The strongest *P. crispum* SDH inhibitor was tannic acid (Fig. 7). Tannins have strong astringent properties, which may induce complexation with enzymes and substrates (Tintino et al., 2016). They bind to proteins (by hydrophobic, hydrophilic, non-specific, and specific interactions), pigments, low-molecular-weight compounds, and metallic ions (Kato et al., 2017). In microorganisms, interactions between tannic acid and the cell membrane can affect its permeability through the inhibition of the efflux pump, which may be associated with an antimicrobial effect (Tintino et al., 2016). Furthermore, the potentially extracellular localization of tannic acid may contribute to this effect because leaf mesophyll cell walls are the typical site of origin and deposition of hydrolysable tannins in oak leaves (Grundhofer et al., 2001). Furthermore, in the outer peels of pomegranate (*Punica granatum* L.), SDHs play a role in controlling the biosynthesis of hydrolysable tannins (Habashi et al., 2019).

Our results also showed that *P. crispum* SDH is inhibited at 0.15 and 0.19 mM IC_{50} by caffeic acid and chlorogenic acid (with 2 and 5 hydroxyl groups in the structure), respectively (Fig. 7). Chlorogenic acids are esters formed between caffeic acid and quinic acid, which are strong antioxidants found in many vegetable species and coffee beans (Colon and Nerin, 2016; Guo et al., 2014; Liang and Kitts, 2015; Niggeweg et al., 2004). In plants, chlorogenic acids serve as protecting compounds against stress, e.g., viral infection (Spoustova et al., 2015), or as feeding deterrents (Ikonen et al., 2001). The *p*-coumaric, *t*-ferulic, sinapic, syringic, and salicylic acids, all with only one hydroxyl group, were milder SDH inhibitors, with IC_{50} above 5 mM, and they are not involved in regulation under physiological conditions. Salicylic acid is an important signal molecule; however, its concentration does not reach the value of the experimentally determined IC_{50}, even during stress (Belonoznikova et al., 2020). In their

study, Belinsky and Davies concluded that the both carbonyl group at the C1 position and a hydroxyl group at the 4-OH position are significant determinants of ligand binding. This is true for syringic acid with IC_{50} 5.1 ± 1.0 mM. Tannic acid contains several hydroxyl groups on phenyl rings; thus, their hydroxyl groups may interact with the amino acid residue in the enzyme active center.

Under non-stress conditions, plant SDH may be inhibited by some phenylpropanoid compounds. In our previous study, we found significant chlorogenic and quinic acid depletion in tobacco plants exposed to potyviral stress and heat shock (Hyskova et al., 2021). Such a depletion could in turn favor the shikimate pathway, producing precursors of defense compounds by enhancing SDH activity.

Plant SDH inhibition by divalent metal ions, particularly Zn^{2+} and Cu^{2+}, is known and correlated with the inactivation of functional sulfhydryl groups of SDH and also confirmed with the inhibition of plant SDH by *p*-chloromercuribenzoate which could be reversed by cysteine (Balinsky and Davies, 1961; Koshiba, 1978; Lourenco and Neves, 1984). SDH from *P. crispum* root was also inhibited by Zn^{2+} and Cu^{2+}, particularly by Cu^{2+} ions (Table 4).

4. Conclusions

P. crispum root SDH follows an ordered reaction mechanism with three dead-end complexes in both directions. PCA was identified as a side product of SDH, whereas GA was formed non-enzymatically and quinate was not detected. As such, the phenylpropanoid pathway leading to the synthesis of precursors of monolignols (initiating with cinnamic acid and continuing with *p*-coumaric acid, caffeic acid, ferulic acid, 5-hydroxyferulic and sinapic acid) affects SDH activity through feedback regulation. Moreover, their number of hydroxyl groups increases their inhibition effect on SDH. Accordingly, tannic acid, chlorogenic acid,

and caffeic acid are the most effective inhibitors of *P. crispum* root SDH, which may be feedback-regulated by phenylpropanoids under stress conditions.

5. Material and methods

5.1. Extraction and Purification of SDH

The plants (vegetables?) *P. crispum*, *Cucurbita pepo* L. var. cylindrica (Cucurbitaceae), *Cucurbita pepo* L. var. pepo (Cucurbitaceae), *Apium graveolens* L. var. rapaceum (Apiaceae), *Daucus carota* subsp. sativus (Apiaceae), *Brassica oleracea* var. italica (Brassicaceae), and **Allium cepa** L. (Amaryllidaceae) were purchased from the farmer company Bramko s.r.o. in the Czech Republic. All the plants were grown in the fields. *Zingiber officinale* L. (Zingiberaceae) was purchased from the Nature's promise company, previously grown in China. The amount of 1 g of each vegetable (P. crispum root, zucchini and pumpkin fruit, celery, ginger, carrot, broccoli, or onion) was homogenized in 3 ml of 100 mM Tris-HCl, pH 7.8 buffer containing 1 mM dithiothreitol, 1 mM EDTA, 5 mM $MgCl_2$, and 5 % (v/v) glycerol) with 0.02 g/ml of poly(vinylpyrrolidone) and centrifuged at 16600*g* for 15 min. The supernatant was used to measure SDH activity. SDH was purified from 100 g of *P. crispum* root by ammonium sulfate precipitation, ion exchange chromatography on DEAE-cellulose, and gel filtration on Sephacryl S-300, as described previously (Ryšlavá et al., 2007).

5.2. SDH activity assay

SDH activity was monitored spectrophotometrically at 20 °C, following the formation of NADPH during the oxidation of SA into DHS by the increase of absorbance at 340 nm. The SDH assay mixture (total volume of 1 ml) contained 100 mM AMP-NaOH buffer (pH 9.0), 0.2 mM NADP and 3 mM SA. The reaction was initiated by adding the enzyme (50 μl).

Potential regulatory effects of Zn^{2+} (0.1 mM), Cu^{2+} (0.01 mM); Na^{+}, K^{+}, Mg^{2+}, Ca^{2+}, Mn^{2+} and NH_4^{+} (5 mM) ions on SDH activity were tested.

5.3. Determination of pI, pH optimum, and relative molecular weight of SDH

Isoelectric focusing was performed using the Pharmacia system FBE-3000 and 125 x 125 mm gels Servalyt, Precotes 3-10, according to the Pharmacia manual, as published previously (Ryšlavá et al., 2007). A standard protein mixture (IEF Markers from Serva with pI 3.5-10.65) was used for calibration. SDH activity was detected by incubating 0.2 mM NADP, 3 mM SA and 10 mg/ml of iodonitroterazolium chloride with 5 μg/ml phenazine methosulfate in 100 mM AMP-NaOH buffer (pH 9.0).

The optimum pH of the enzyme was determined over the following pH ranges: 80 mM MES-NaOH buffer (pH 5.2 – 7.2), 80 mM Tris-HCl buffer (pH 6.8 – 8.6), 80 mM glycine-NaOH buffer (pH 8.6 – 10.6), 80 mM AMP buffer (pH 9.0 – 10.5), 80 mM Na_2CO_3-$NaHCO_3$ buffer (pH 9.5 – 11.0) and 80 mM Na_2HPO_4-NaOH buffer (pH 11.0 – 12.0). SDH activity was measured as described in 2.2.

The relative molecular weight of SDH was determined by gel chromatography on a Sephacryl S-300 column (1.2 x 57 cm). Red native electrophoresis was also used for molecular weight determination (Drab et al., 2011). SDH activity was assessed as described above after isoelectric focusing.

5.4. Determination of kinetic parameters and mechanism of the bisubstrate reaction catalyzed by SDH

The reaction rate was measured by the change of absorbance at 340 nm. In 500 mM Tris-HCl buffer (pH 8), the concentration of one of the substrates ranged from 0.005 to 0.7 mM NADPH and from 0.05 to 2 mM DHS, whereas the saturating concentration of the second substrate DHS and NADPH were 2 mM and 0.7 mM, respectively. The reverse reaction was determined similarly but in 500 mM AMP-NaOH buffer (pH 9.0) with 0.05 – 10

mM NADP and 0.2 – 10 mM SA, whereas the concentration of the second substrate was at saturation, i.e., 10 mM SA and 3 mM NADP, respectively. Kinetic parameters were determined by fitting the data to the Michaelis-Menten Eq. (1) or to an equation characterizing substrate inhibition Eq. (2) and the Michaelis constant (K_m), the maximum reaction rate (V_{max}), the hypothetical maximal reaction rate corresponding to the rate that the enzyme reached in the absence of inhibition by an excess of substrate (V^*_{max}) and the substrate inhibition constant (K_{ss}) were calculated by non-linear regression. All measurements were performed at 20 °C.

$$v = \frac{V_{max}[S]}{K_m + [S]} \qquad \text{Eq. (1)}$$

$$v = \frac{V^*_{max}[S]}{K_m + [S] + \frac{[S]^2}{K_{ss}}} \qquad \text{Eq. (2)}$$

The kinetic mechanism of SDH was studied in both directions by varying the concentration of NADP (0.05-0.5 mM) or NADPH (0.05-0.4 mM) and the concentration of SA (0.2-3 mM) or DHS (0.05-2 mM).

The experimental data of the reaction rate as a function of the substrate (SA, NADP) concentration were fit into general reaction rate equations for the bisubstrate reactions, classified as ping – pong: Eq. (3) and sequential: Eq. (4), and linearization methods, as the double reciprocal plot, Hanes plot or Eadie-Hofstee plot.

$$v = \frac{V_{max}[A][B]}{[B]K_{mA} + [A]K_{mB} + [A][B]} \qquad \text{Eq. (3)}$$

$$v = \frac{V_{max}[A][B]}{[B]K_{mA} + [A]K_{mB} + [A][B] + K_A K_{mB}} \quad \text{Eq. (4)}$$

441

442 V_{max} is the maximal reaction rate of the enzyme reaction, K_{mA} and K_{mB} are the Michaelis
443 constants for the substrate A and B, respectively, and K_A is the dissociation constant for the
444 complex enzyme-substrate. Equations derived for the determination of dead-end complexes
445 are summarized in supplementary material Eq. A.1- A.32.

446 *5.5. Product inhibition study*

447 In the direction from DHS to SA, the reaction mixture contained: 500 mM Tris-HCl
448 buffer (pH 8) and a variable concentration of DHS (0.2; 0.3, 0.5, and 1 mM) or NADPH
449 (0.05; 0.1, 0.2, and 0.3 mM) with a subsaturating concentration of the second substrate, i.e.,
450 0.2 mM NADPH or 0.75 mM DHS. The concentrations of the inhibitors, NADP and SA, were
451 in the 0.1-0.3 mM and 0.5-2 mM ranges, respectively. In this direction, saturating product
452 concentrations could not be measured for technical reasons (NADPH absorbance above 3).

453 In the direction from SA to DHS, the reaction mixture contained: 375 mM AMP-
454 NaOH buffer (pH 9.0) and a variable concentration of SA and NADP. The final variable
455 concentrations of SA (2; 0.5; 0.3; and 0.15 mM) and NADP (0.5; 0.2; 0.1; and 0.05 mM) were
456 tested at saturating and subsaturating concentrations of the second substrate. The saturating
457 concentrations were 20 mM and 2 mM, and the subsaturating concentrations were 0.3 mM
458 and 0.1 mM for SA and NADP, respectively. The concentrations of the inhibitors, NADPH
459 and DHS, were in the 0.05-0.1 and 0.5-1 mM ranges, respectively.

460 The data derived from the product inhibition studies were fitted to the equation
461 describing the relevant type of inhibition: competitive Eq. (5) and non-competitive Eq. (6),
462 where [S] is the substrate concentration, [I] is the inhibitor concentration, and K_{ic} and K_{iu} are
463 the inhibition constants for the inhibitor derived by slope and intercept, respectively, in the
464 Lineweaver-Burk plot.

$$v = \frac{V_{max}[S]}{K_m\left(1+\frac{[I]}{K_{ic}}\right)+[S]} \quad \text{Eq. (5)}$$

$$v = \frac{V_{max}[S]}{K_m\left(1+\frac{[I]}{K_{ic}}\right)+\left(1+\frac{[I]}{K_{iu}}\right)[S]} \quad \text{Eq. (6)}$$

5.6. Identification of all SDH products

SDH isolated from *P. crispum* root (10 µl with specific activity 470 nmol.min^{-1}.mg^{-1}) was incubated in the 280 µL reaction mixture containing either 100 mM Tris-HCl pH 8 (in the physiological direction, see Fig. 6) or 100 mM AMP-NaOH pH 9 buffers, 0.14 mM NADP(H)/NAD(H) and 2 mM SA/DHS/DHQ/QA/GA/PCA for 30 min at 20 °C. The reaction was initiated by adding the enzyme and stopped by adding 10 µl of 99 % (v/v) formic acid. Blank experiments were prepared similarly, albeit adding formic acid before the enzyme. The calibration standards were purchased from Sigma-Aldrich (USA) and Carl Roth (Germany).

The reaction mixtures were assayed by reversed-phase liquid chromatography coupled to electrospray mass spectrometry (LC-MS). The injection volume was 5 µL (Dionex UltiMate 3000, Thermo Fisher Scientific, USA). A Zorbax C18 reversed-phase silica-based column was used for all separations (150 × 2.1 mm, 3.5 µm, Agilent, USA). The mobile phase consisted of 0.5 % (v/v) formic acid in 10 % (v/v) acetonitrile in water (eluent A); and 0.3 % (v/v) formic acid in 100 % (v/v) acetonitrile (eluent B). The flow rate was set to 0.250 ml/min at 37 °C. The following elution program was used: isocratic A for 7 min, 0-100 % B for 1 min, isocratic B for 2 min, isocratic A for 3 min. MS analysis was performed on a ESI-Q-TOF maXis II (Bruker, USA). All mass spectrometric data were acquired in negative ionization mode.

5.7. Effect of secondary metabolites on the SDH

Selected secondary metabolites were tested for their potential regulatory effect on SDH activity. The reversibility of inhibition by these compounds was tested simultaneously (Appendix A Supplementary material). Tannic acid was dissolved in distilled water, caffeic acid, chlorogenic acid, *t*-ferulic acid, *p*-coumaric acid, and salicylic acid were dissolved in 96 % ethanol, and sinapic and syringic acids were dissolved in 50 % ethanol. The final concentration of ethanol did not affect SDH activity. Since phenylpropanoids interfered with the spectrophotometric assay (increasing absorbance at 340 nm), this assay was replaced with the colorimetric microplate method. A reaction mixture (280 ul) consisting of 180 mM AMP-NaOH buffer (pH 9.0), 0.14 mM NADP, 2.1 mM SA, 5 mg/ml iodonitrotetrazolium with 5 µg/ml phenazine methosulfate, and 20 µl of potential inhibitor compound was incubated with 10 µl of enzyme for 15 minutes. The reaction was terminated with 10 µl of 99 % formic acid, measuring the absorbance at 500 nm.

Simultaneously, blank reactions were prepared in which 10 µl of enzyme was first treated with 10 µl of 99 % (v/v) formic acid and then with the reaction mixture. Another blank was prepared as the individual reaction (including incubation time), albeit replacing the enzyme with distilled water.

The half maximal inhibitory concentration IC_{50} was calculated from Eq. (7). [I] is the inhibitor concentration, a and b are the maximal and minimal values of reaction rate, respectively, and c corresponds to the slope of the sigmoid function.

$$v = b + \frac{a - b}{1 + \left(\frac{[I]}{IC_{50}}\right)^{c}} \qquad \text{Eq. (7)}$$

5.8. Determination of protein and total phenolic content

Soluble proteins were determined according to Bradford (Bradford, 1976), and total phenolics compounds were quantified according to Tupec et al. (Tupec et al., 2017).

5.9. Statistics

SDH isolation was performed in 20 independent biological replicates, repeating each measurement at least three times. Data were analyzed and processed in SigmaPlot v. 12 (Systat Software, Inc.) and Microsoft Excel 2019 (Microsoft Corp.).

Table 1 Kinetic parameters of *P. crispum* SDH

V_{max} - maximal reaction rate of enzyme reaction, K_m- Michaelis constant of the specific substrate, K'_m -apparent Michaelis constant at a given concentration of the second substrate), K_{SS} - inhibition constant at an excess substrate concentration, K_A - dissociation constant of the enzyme – substrate complex, ♣for technical reasons (absorbance above 3 or excess substrate inhibition), this parameter could not be determined. Kinetic constants were calculated as an average of values from at least 3 experiments performed in doublets, S. D. are shown.

	Direction of the reaction catalyzed by SDH	
	SA → DHS	**DHS → SA**
pH optimum	9.5-10	7-8.5
V_{max} [μmol.min^{-1}.mg^{-1}] for SA (DHS)	1.34	0.29
V_{max} [μmol.min^{-1}.mg^{-1}] for NADP(H)	1.32	0.28
K_m for SA (DHS) [mM]	0.71 ± 0.13	♣

K_m for NADP(H) [mM]	0.47 ± 0.16	♣
K'_m for SA (with 0.2 mM NADP)	0.16 ± 0.01	-
K'_m for DHS (with 0.4 mM NADPH)	-	0.23 ± 0.03
K'_m for NADP (with 3 mM SA)	0.054 ± 0.011	-
K'_m for NADPH (with 2 mM DHS)	-	0.016 ± 0.03
K_{SS} for SA (DHS) [mM]	-	0.12 ± 0.07
K_A	0.030 ± 0.008	0.25 ± 0.13

529

530

Table 2 Results of the product inhibition study for the determination of the bisubstrate reaction mechanism of *P. crispum* SDH. Inhibition constants were calculated as an average of values from 2-4 experiments carried out in doublets, S.D. are shown.

Patterns and values in brackets mean that the reaction is saturated with the 2nd substrate.

	Product inhibitor				Product inhibitor			
	Q (NADP)		P (SA)		A (NADPH)		B (DHS)	
	Varied substrate				Varied substrate			
i.e.	1/NADPH	1/DHS	1/NADPH	1/DHS	1/NADP	1/SA	1/NADP	1/SA
2nd substrate	subsaturated				subsaturated (saturated)			
Pattern	C	NC	C	NC	C (C)	NC (N.I.)	NC (N.I.)	C (C)
Ki [mM]	0.22±0.02	0.4±0.1	0.7±0.1	0.7±0.3	0.12±0.07 (0.49±0.03)	0.36± 0.08	1.4±0.2	0.13±0.03 (0.33±0.03)
Mechanism	steady state sequential order				steady state sequential order			

538 **Table 3 Identification of SDH products by LC-MS analysis.** List of products detected after
539 30 min incubation with (and without) SDH enzyme at 20 °C. DHS, 3-dehydroshikimate; DHQ,
540 3-dehydroquinate; PCA, protocatechuic acid; SA, shikimic acid; QA, quinate. *the incubation
541 time was 60 min at 20 °C. Each determination was done at least 3-times, the average values and
542 S.D. are shown.

reaction	**products [nmol]**
SA+NADP	DHS: 5.7 ± 0.7
	PCA: 0.1 ± 0.0
*DHS+NADPH	SA: 4.9 ± 0.2
	GA: 0.5 ± 0.0
	PCA: 0.7 ± 0.1
	DHQ: 1.1 ± 0.0
DHS+NADP	GA: 0.1 ± 0.0
	PCA: 0.3 ± 0.2
DHS+NADP	GA: 2.1 ± 0.4
– without SDH	PCA: 2.7 ± 0.6
DHQ+ NADP	DHS: 17.4 ± 1.4
	PCA: 4.9 ± 0.4
*DHQ+ NADPH	DHS: 3.4 ± 0.8
	SA: 1.4 ± 0.2
	GA: 1.1 ± 0.5
	PCA: 1.3 ± 0.2
DHQ+NADH	No products detected.
QA+NAD	No products detected.
PCA+NADPH	No products detected.

543
544

Table 4 The effect of various ions on *P. crispum* SDH activity. Screening was performed spectrophotometrically at 340 nm in the presence of 3 mM SA, 0.2 mM NADP and 5 mM*, 0.1 mM**, or 0.01 mM*** concentration of potential modulator. Each determination was done at least 3-times, the average values and S.D. are shown.

Compound	**% of activity**
$(NH_4)_2SO_4$	115.6±9.8 *
$CaCl_2$	113.2±8.2 *
NaCl	105.2±3.7 *
KCl	107.0±7.3 *
$MgCl_2$	99.3±15.0 *
$MnCl_2$	77.6±23.1 *
$ZnSO_4$	10.1±4.8 **
$CuSO_4$	21.2±8.3 ***

553 **Figures**

554 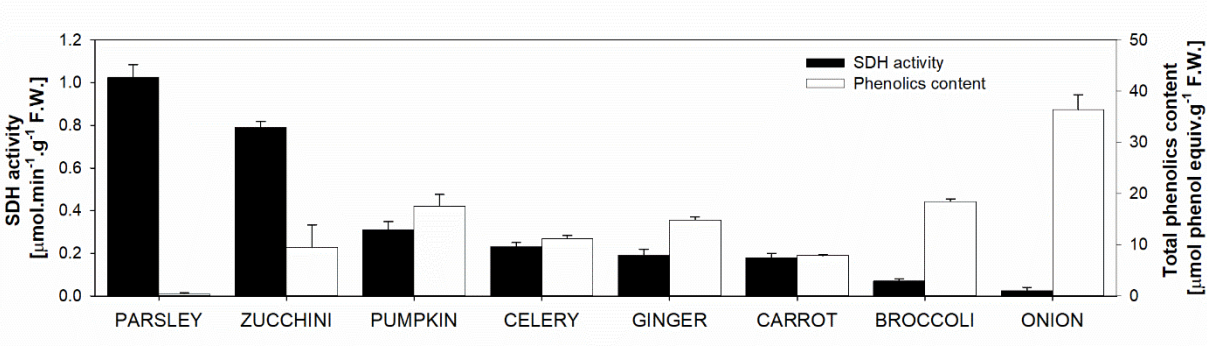

555 **Fig. 1 Searching for plant sources of SDH activity**. High SDH activity (black columns)
556 correlates with low total phenolics content (white columns) and *vice versa*. Each determination
557 was done at least 3-times, the average values and S.D. are shown.

558

559

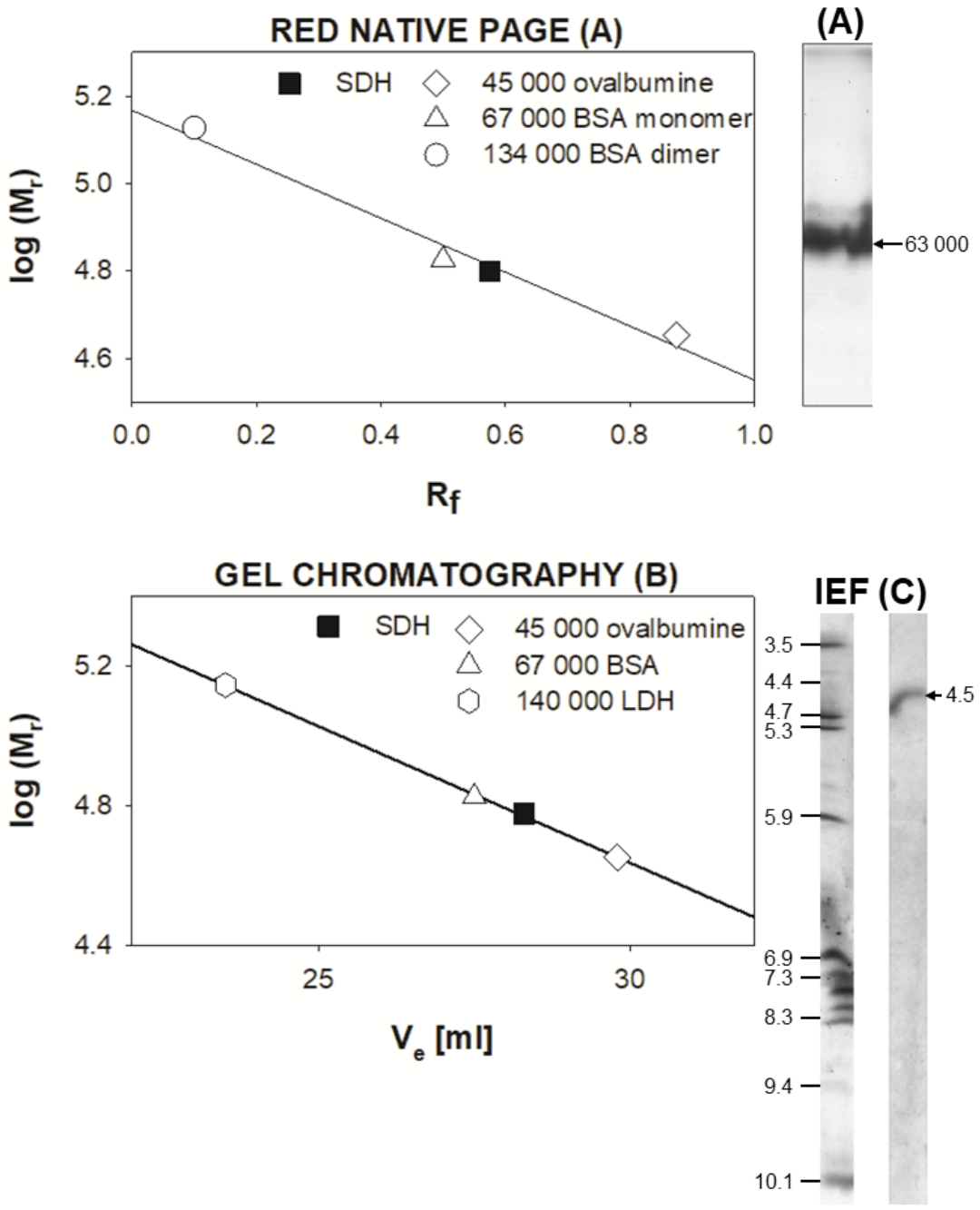

560

561 **Fig. 2 Estimation of the relative molecular mass of SDH** using red native PAGE (A) and

562 gel chromatography on a Sephacryl-S300 column (B) and determination of pI using

563 isoelectric focusing (C). The arrows indicate the position of SDH. R_f corresponds to the

564 retention factor.

565

566

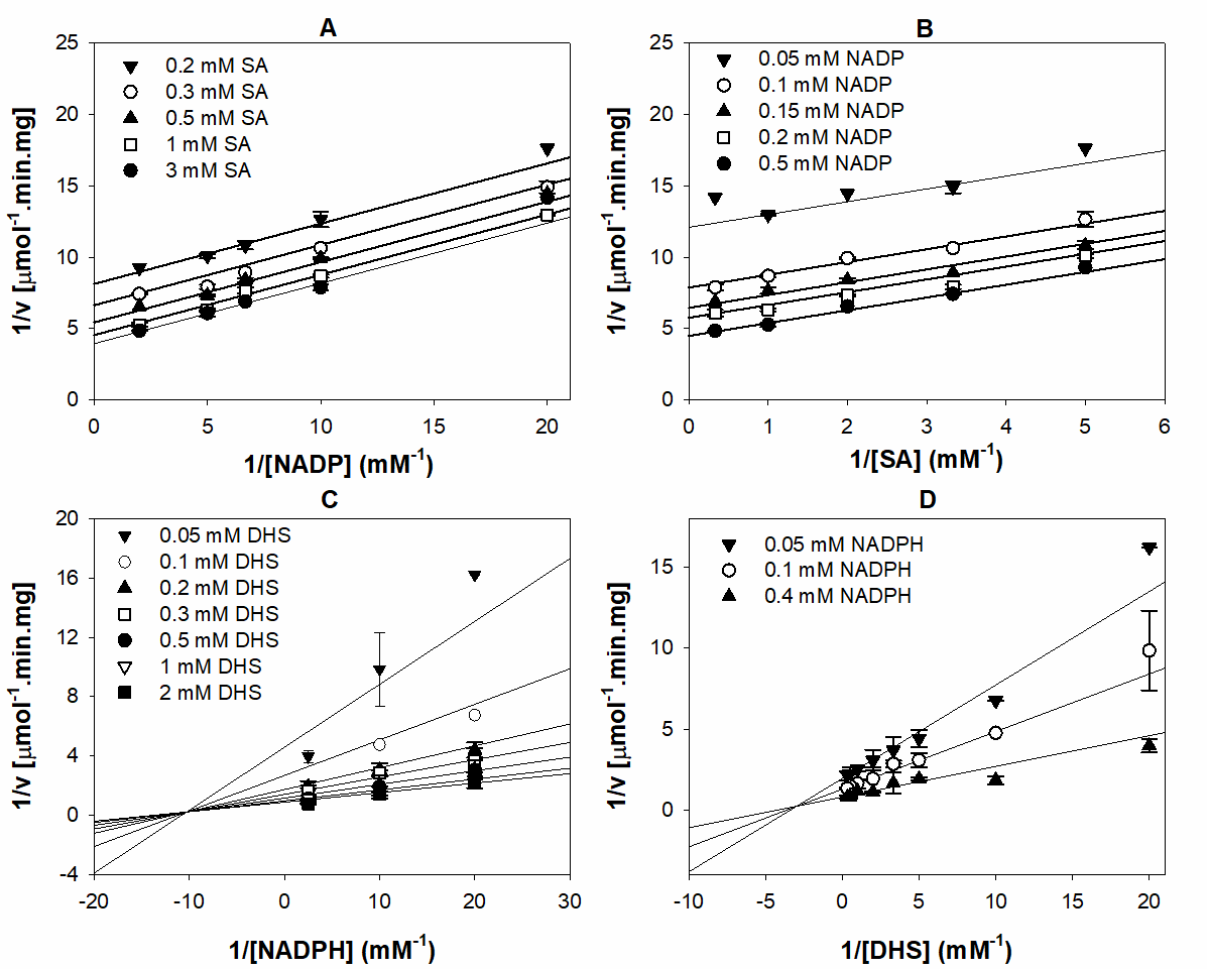

Fig. 3 Determination of the type of SDH reaction mechanism based on Lineweaver-Burk diagnostical plots for the direction from SA to DHS (A,B) and from DHS to SA (C,D)

Double reciprocal plots are fitted to an equation corresponding to a sequential mechanism.

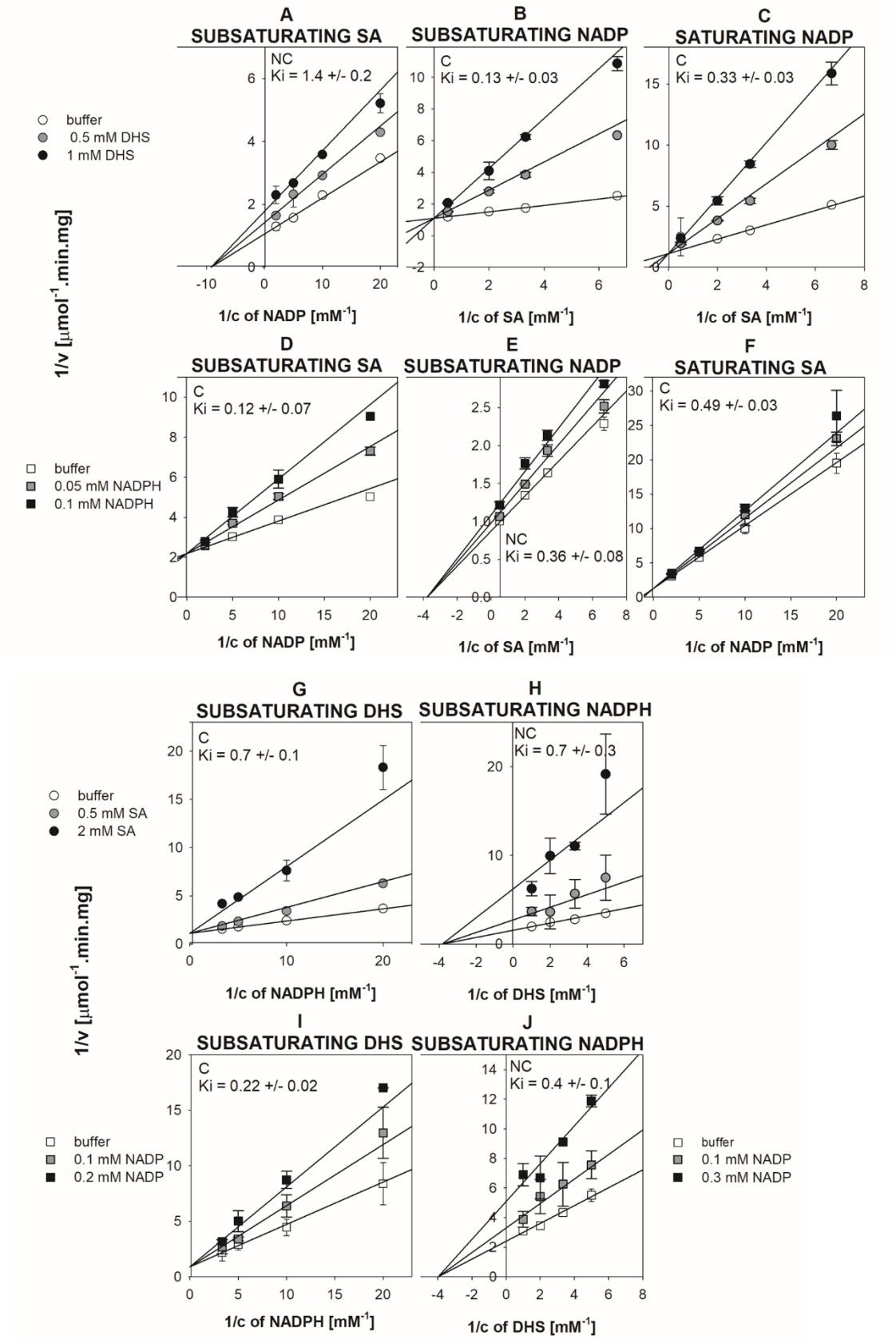

Fig. 4 Product inhibition analysis for the determination of the mechanism of bisubstrate reaction in the direction from SA to DHS (A-F) and in the direction from DHS to SA (G-

574 **J**). Experimental data are fitted with calculated values determined by non-linear regression
575 using equations charactering competitive and non-competitive inhibition, respectively. SDH
576 products DHS (A,B,C) and NADPH (D,E,F) served as competitive (B,C,D,F) and non-
577 competitive (A,E) inhibitors. The saturating (C,F) and subsaturating (A,B,D,E) concentrations
578 of SA and NADP were 20 mM and 2 mM, and 0.3 (2) mM and 0.5 mM, respectively.
579 Saturating concentrations of NADP and variable concentrations of SA caused no inhibition
580 (N.I.) of NADPH and saturating concentrations of SA and variable concentrations of NADP
581 caused N.I. of DHS (data not shown). SDH products SA (G,H) and NADP (I,J) served as
582 competitive (G,I) and non-competitive (H,J) inhibitors at 0.75 mM (subsaturating
583 concentration) DHS (G,I) and 0.2 mM (subsaturating concentration) NADPH (H,J) as a
584 second substrate. K_i indicates inhibition constants in mM. Measurements were performed in
585 doublets (S.D. are shown) and at least 2-4 times (enzyme preparations from different
586 isolations).

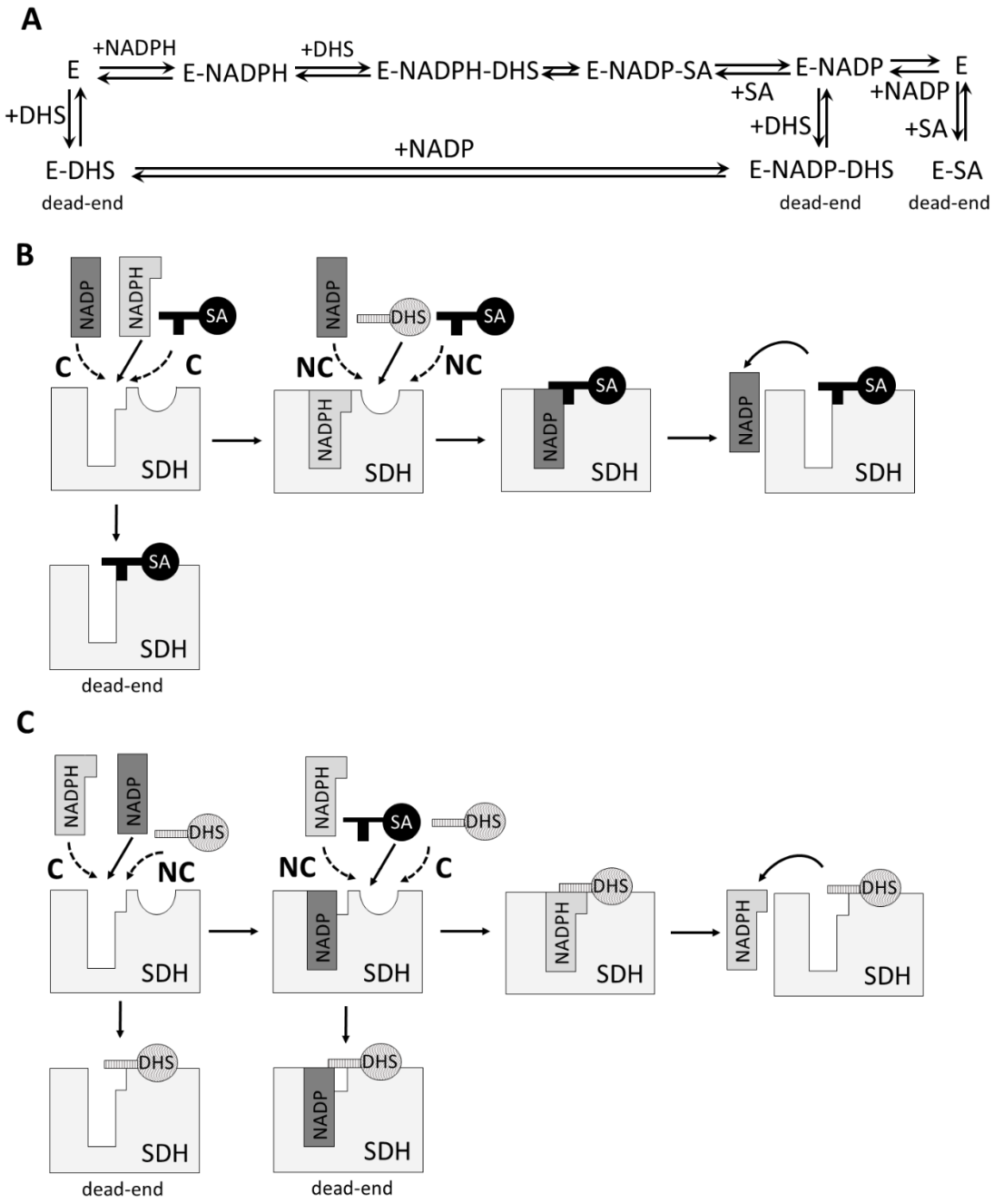

587

588 **Fig. 5 Proposed kinetic mechanism of the bisubstrate reaction catalyzed by *P. crispum***

589 **SDH from non-photosynthetic tissue**. SDH reaction scheme (A), graphical representation of

590 the product inhibition study in DHS reduction direction (B) and in SA oxidation direction (C)

591 with a formation of dead-end complexes. Non-Competitive (NC) and competitive (C) product

592 inhibitors are indicated.

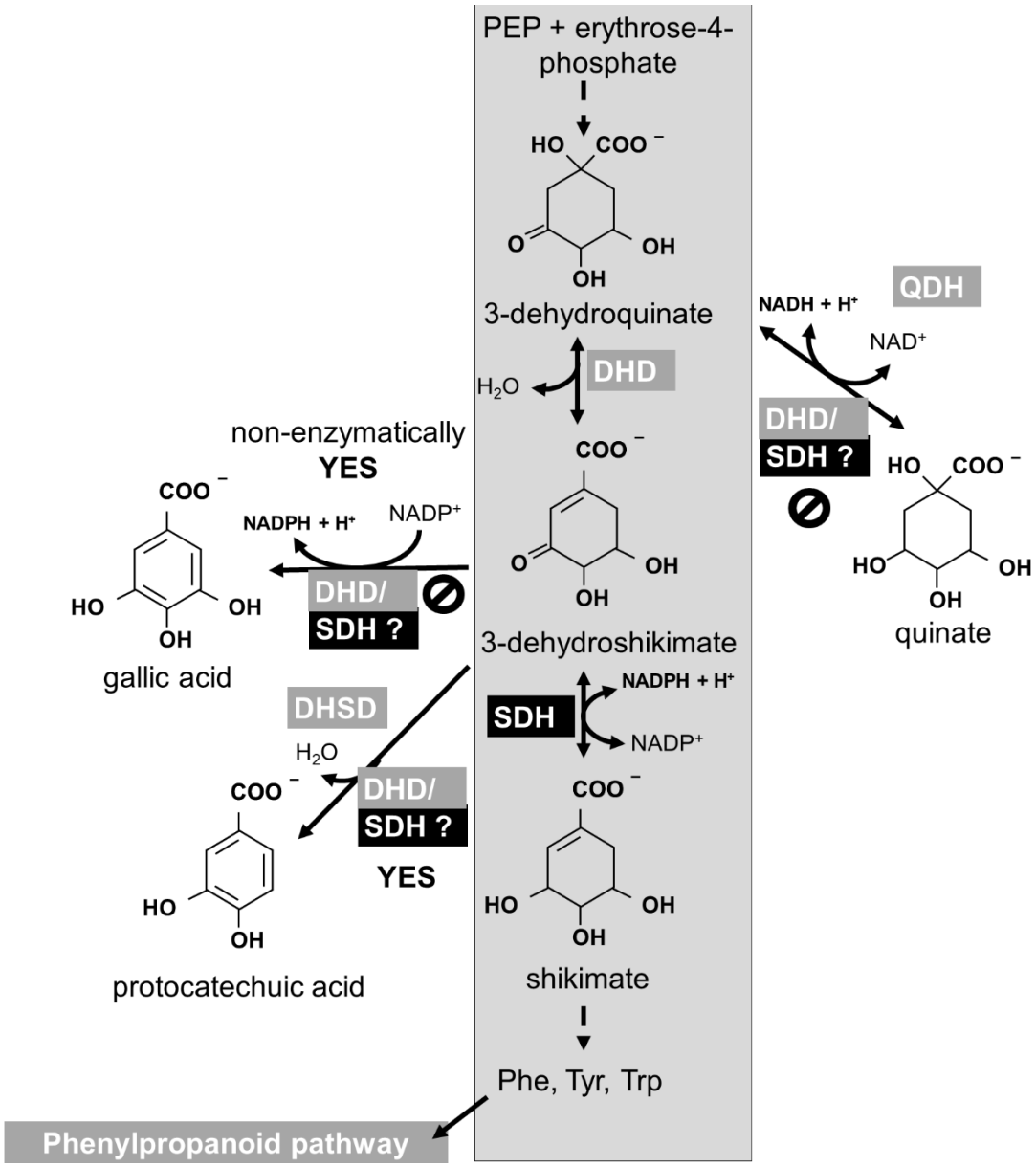

593

594 **Fig. 6 Identification of *P. crispum* SDH products by reversed-phase liquid**

595 **chromatography coupled to electrospray mass spectrometry**. The symbol ∅ indicates that

596 no potential *P. crispum* SDH byproduct was identified in the reaction mixtures by mass

597 spectrometry. QDH, quinate dehydrogenase; QD, quinate dehydratase; DHSD,

598 dehydroshikimate dehydratase.

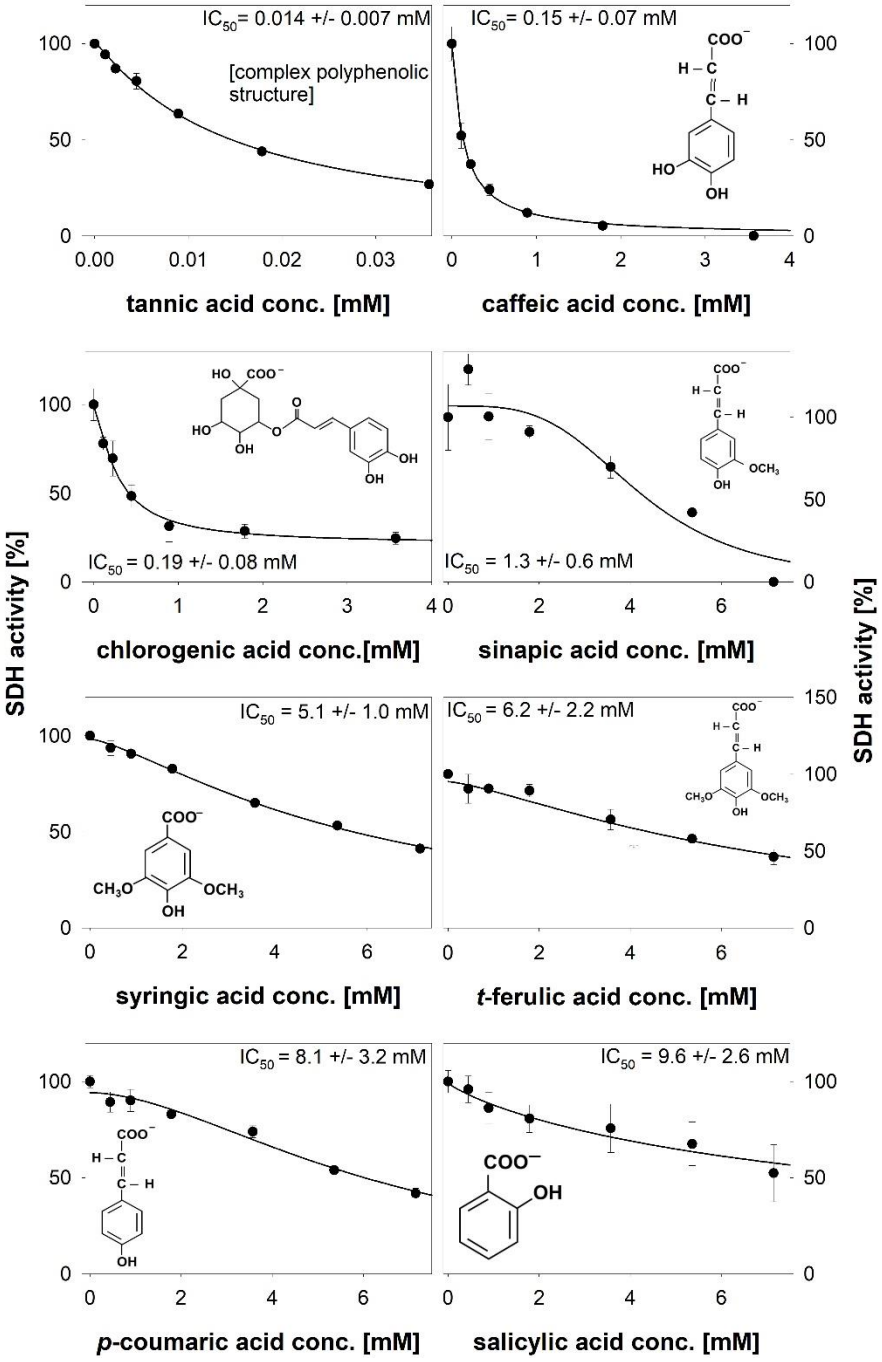

Fig. 7 Inhibition effect of various phenylpropanoids on the activity of *P. crispum* SDH.

The specific activity of the enzyme preparations was 0.17 ± 0.07 μmol.min^{-1}mg^{-1}. Controls in 96 and 50 % ethanol were only slightly different from the distilled water control, with specific activities of 0.18 ± 0.06 and 0.19 ± 0.11 μmol.min^{-1}mg^{-1}, respectively. IC_{50} was calculated from

nonlinear regression with Eq. (7). Each determination was done at least 3-times, the average values and standard deviations are shown.

Declaration of competing interest

The authors declare that they have no known competing financial interests or personal relationships that could have appeared to influence the work reported in this table.

Author Contributions: V.H. conceptualization, data curation, formal analysis, investigation, resources, writing-original draft, K.B. investigation, data curation, methodology, validation, formal analysis, funding acquisition, writing-original draft, I.S. investigation, D.K. investigation, data curation, and methodology, M.I. software, validation, writing-review and editing, H.R. supervision, project administration, funding acquisition, resources, writing-review and editing.

Acknowledgement: This work was supported (in part) by Charles University (SVV260572/2020). The authors thank Dr. Carlos V. Melo for English editing the manuscript.

Reference

Avitia-Dominguez, C., Sierra-Campos, E., Salas-Pacheco, J. M., Najera, H., Rojo-Dominguez, A., Cisneros-Martinez, J., Tellez-Valencia, A., 2014. Inhibition and biochemical characterization of methicillin-resistant *Staphylococcus aureus* shikimate dehydrogenase: an in silico and kinetic study. Molecules 19, 4491-4509. https://doi.org/10.3390/molecules19044491.

Baillie, A. C., Corbett, J. R., Dowsett, J. R., McCloskey, P., 1972. Inhibitors of shikimate dehydrogenase as potential herbicides. Pestid. Sci. 3, 113-120. https://doi.org/10.1002/ps.2780030202.

Balinsky, D., Davies, D. D., 1961. Aromatic biosynthesis in higher plants. 1. Preparation and properties of dehydroshikimic reductase. Biochem. J. 80, 292-296. https://doi.org/10.1042/bj0800292.

Balinsky, D., Dennis, A. W., Cleland, W. W., 1971. Kinetic and isotope-exchange studies on shikimate dehydrogenase from *Pisum sativum*. Biochemistry 10, 1947-1952. https://doi.org/10.1021/bi00786a032.

Belonoznikova, K., Vaverova, K., Vanek, T., Kolarik, M., Hyskova, V., Vankova, R., Dobrev, P., Krizek, T., Hodek, O., Cokrtova, K., Stipek, A., Ryslava, H., 2020. Novel insights into the effect of Pythium strains on rapeseed metabolism. Microorganisms 8, doi: 10.3390/microorganisms8101472. https://doi.org/10.3390/microorganisms8101472.

Bontpart, T., Marlin, T., Vialet, S., Guiraud, J. L., Pinasseau, L., Meudec, E., Sommerer, N., Cheynier, V., Terrier, N., 2016. Two shikimate dehydrogenases, VvSDH3 and VvSDH4, are involved in gallic acid biosynthesis in grapevine. J. Exp. Bot. 67, 3537-3550. https://doi.org/ 10.1093/jxb/erw184.

Bradford, M. M., 1976. A rapid and sensitive method for the quantitation of microgram quantities of protein utilizing the principle of protein-dye binding. Anal. Biochem. 72, 248-254. https://doi.org/210.1006/abio.1976.9999.

Buchanan, B. B., Gruissem, W., L.Jones, R., 2000. Biochemistry & Molecular Biology of Plants. American Society of Plant Physiologists, Rockville, Maryland.

Cabane, M., Pireaux, J. C., Leger, E., Weber, E., Dizengremel, P., Pollet, B., Lapierre, C., 2004. Condensed lignins are synthesized in poplar leaves exposed to ozone. Plant Physiol. 134, 586-594. https://doi.org/ 10.1104/pp.103.031765.

Carrington, Y., Guo, J., Le, C. H., Fillo, A., Kwon, J., Tran, L. T., Ehlting, J., 2018. Evolution of a secondary metabolic pathway from primary metabolism: shikimate and quinate biosynthesis in plants. Plant J. 95, 823-833. https://doi.org/ 10.1111/tpj.13990.

Colon, M., Nerin, C., 2016. Synergistic, antagonistic and additive interactions of green tea polyphenols. Eur. Food Res. Technol. 242, 211–220. https://doi.org/ 10.1007/s00217-015-2532-9.

Deng, Y., Lu, S., 2017. Biosynthesis and regulation of phenylpropanoids in plants. Crit. Rev. Plant Sci. 36, 257-290. https://doi.org/10.1080/07352689.2017.1402852.

Derrer, B., Macheroux, P., Kappes, B., 2013. The shikimate pathway in apicomplexan parasites: implications for drug development. Front. Biosci. 18, 944-969. https://doi.org/ 10.2741/4155

Diaz-Quiroz, D. C., Cardona-Felix, C. S., Viveros-Ceballos, J. L., Reyes-Gonzalez, M. A., Bolivar, F., Ordonez, M., Escalante, A., 2018. Synthesis, biological activity and molecular modelling studies of shikimic acid derivatives as inhibitors of the shikimate dehydrogenase enzyme of *Escherichia coli*. J. Enzyme Inhib. Med. Chem. 33, 397-404.

https://doi.org/ 10.1080/14756366.2017.1422125.
Diaz, J., Merino, F., 1997. Shikimate dehydrogenase from pepper (*Capsicum annuum*) seedlings. Purification and properties. Physiol. Plantarum 100, 147-152. https://doi.org/10.1111/j.1399-3054.1997.tb03465.x.
Dowsett, J. R., Middleton, B., Corbett, J. R., Tubbs, P. K., 1972. The anomalous inhibition of shikimate dehydrogenase by analogues of dehydroshikimate. Biochim. Biophys. Acta 276, 344-349. https://doi.org/ 10.1016/0005-2744(72)90994-1.
Drab, T., Kracmerova, J., Ticha, I., Hanzlikova, E., Ticha, M., Ryslava, H., Doubnerova, V., Manaskova-Postlerova, P., Liberda, J., 2011. Native red electrophoresis--a new method suitable for separation of native proteins. Electrophoresis 32, 3597-3599. https://doi.org/ 10.1002/elps.201100310.
Esposito, S., Carfagna, S., Massaro, G., Vona, V., Di Martino Rigano, V., 2001. Glucose-6-phosphate dehydrogenase in barley roots: kinetic properties and localisation of the isoforms. Planta 212, 627-634. https://doi.org/ doi: 10.1007/s004250000443.
Esposito, S., Massaro, G., Vona, V., Di Martino Rigano, V., Carfagna, S., 2003. Glutamate synthesis in barley roots: the role of the plastidic glucose-6-phosphate dehydrogenase. Planta 216, 639-647. https://doi.org/ 10.1007/s00425-002-0892-4.
Fiedler, E., Schultz, G., 1985. Localization, purification, and characterization of shikimate oxidoreductase-dehydroquinate hydrolyase from stroma of spinach chloroplasts. Plant Physiol. 79, 212-218. https://doi.org/ 10.1104/pp.79.1.212.
Fonseca, I. O., Silva, R. G., Fernandes, C. L., de Souza, O. N., Basso, L. A., Santos, D. S., 2007. Kinetic and chemical mechanisms of shikimate dehydrogenase from *Mycobacterium tuberculosis.* Arch. Biochem. Biophys. 457, 123-133. https://doi.org/ 10.1016/j.abb.2006.11.015.
Garcia-Guevara, F., Bravo, I., Martinez-Anaya, C., Segovia, L., 2017. Cofactor specificity switch in shikimate dehydrogenase by rational design and consensus engineering. Protein Eng. Des. Sel. 30, 533-541. https://doi.org/ 10.1093/protein/gzx031.
Grundhofer, P., Niemetz, R., Schilling, G., Gross, G. G., 2001. Biosynthesis and subcellular distribution of hydrolyzable tannins. Phytochemistry 57, 915-927. https://doi.org/ 10.1016/s0031-9422(01)00099-1.
Guo, J., Carrington, Y., Alber, A., Ehlting, J., 2014. Molecular characterization of quinate and shikimate metabolism in *Populus trichocarpa*. J. Biol. Chem. 289, 23846-23858. https://doi.org/ 10.1074/jbc.M114.558536.
Habashi, R., Hacham, Y., Dhakarey, R., Matityahu, I., Holland, D., Tian, L., Amir, R., 2019. Elucidating the role of shikimate dehydrogenase in controlling the production of anthocyanins and hydrolysable tannins in the outer peels of pomegranate. BMC Plant Biol. 19, 476-491. https://doi.org/410.1186/s12870-12019-12042-12871.
Han, C., Wang, L., Yu, K., Chen, L., Hu, L., Chen, K., Jiang, H., Shen, X., 2006. Biochemical characterization and inhibitor discovery of shikimate dehydrogenase from *Helicobacter pylori.* FEBS J. 273, 4682-4692. https://doi.org/ 10.1111/j.1742-4658.2006.05469.x.
Heldt, H.-W., Piechulla, B., Heldt, F., 2011. Plant Biochemistry-Translation of the 4th German edition. Elsevier Academic Press, Amsterdam, Boston, Heildelberg, London, New York, Oxford, Paris, San Diego, San Francisco, Singapore, Sydney, Tokyo.

Huang, K., Li, M., Liu, Y., Zhu, M., Zhao, G., Zhou, Y., Zhang, L., Wu, Y., Dai, X., Xia, T., Gao, L., 2019. Functional analysis of 3-dehydroquinate dehydratase/shikimate dehydrogenases involved in shikimate pathway in Camellia sinensis. Front. Plant Sci. 10, doi: 10.3389/fpls.2019.01268.
https://doi.org/10.3389/fpls.2019.01268

Hyskova, V., Belonoznikova, K., Doricova, V., Kavan, D., Gillarova, S., Henke, S., Synkova, H., Ryslava, H., Cerovska, N., 2021. Effects of heat treatment on metabolism of tobacco plants infected with *Potato virus Y*. Plant Biol. doi: 10.1111/plb.13234.
https://doi.org/10.1111/plb.13234

Hyskova, V., Pliskova, V., Cerveny, V., Ryslava, H., 2017. NADP-dependent enzymes are involved in response to salt and hypoosmotic stress in cucumber plants. Gen. Physiol. Biophys. 36, 247-258.
https://doi.org/ 10.4149/gpb_2016053.

Ikonen, A., Tahvanainen, J., Roininen, H., 2001. Chlorogenic acid as an antiherbivore defence of willows against leaf beetles. Entomol. Exp. Appl. 99, 47–54.
https://doi.org/10.1046/j.1570-7458.2001.00800.x.

Kambourakis, S., Frost, J. W., 2000. Synthesis of gallic acid: Cu(2+)-mediated oxidation of 3-dehydroshikimic acid. J. Org. Chem. 65, 6904-6909.
https://doi.org/ 10.1021/jo000335z.

Kato, C. G., Goncalves, G. A., Peralta, R. A., Seixas, F. A. V., de Sa-Nakanishi, A. B., Bracht, L., Comar, J. F., Bracht, A., Peralta, R. M., 2017. Inhibition of alpha-amylases by condensed and hydrolysable tannins: focus on kinetics and hypoglycemic actions. Enzyme Res. 2017, doi: 10.1155/2017/5724902.
https://doi.org/ 10.1155/2017/5724902.

Kolarovic, J., Popovic, M., Zlinska, J., Trivic, S., Vojnovic, M., 2010. Antioxidant activities of celery and parsley juices in rats treated with doxorubicin. Molecules 15, 6193-6204.
https://doi.org/ 10.3390/molecules15096193.

Koshiba, T., 1978. Purification of two forms of the associated 3-dehydroquinate hydro-lyase and shikimate:NADP+ oxidoreductase in *Phaseolus mungo* seedlings. Biochim. Biophys. Acta 522, 10-18.
https://doi.org/ 10.1016/0005-2744(78)90317-0.

Kovacik, J., Klejdus, B., Backor, M., 2009. Phenolic metabolism of *Matricaria chamomilla* plants exposed to nickel. J. Plant Physiol. 166, 1460-1464.
https://doi.org/ 10.1016/j.jplph.2009.03.002.

Lemos Silva, G. M., Lourenco, E. J., Neves, V. A., 1985. Inhibition of shikimate dehydrogenase from heart-of-palm (*Euterpe oleracea* Mart.). J. Food Biochem. 9, 105-116. https://doi.org/10.1111/j.1745-4514.1985.tb00342.x.

Liang, N., Kitts, D. D., 2015. Role of chlorogenic acids in controlling oxidative and inflammatory stress conditions. Nutrients 8, doi:10.3390/nu8010016.
https://doi.org/ 10.3390/nu8010016.

Lourenco, E. J., Neves, V. A., 1984. Partial purification and some properties of shikimate dehydrogenase from tomatoes. Phytochemistry 23, 497-499.
https://doi.org/10.1016/S0031-9422(00)80366-0.

Lourenco, E. J., Silva, G. M., Neves, V. A., 1991. Purification and properties of shikimate dehydrogenase from cucumber (*Cucumis sativus* L.). J. Agric. Food Chem. 39, 458-462.
https://doi.org/ https://doi.org/10.1021/jf00003a006.

Moura, J. C., Bonine, C. A., de Oliveira Fernandes Viana, J., Dornelas, M. C., Mazzafera, P., 2010. Abiotic and biotic stresses and changes in the lignin content and composition in plants. J. Integr. Plant Biol. 52, 360-376.
https://doi.org/ 10.1111/j.1744-7909.2010.00892.x

Muir, R. M., Ibanez, A. M., Uratsu, S. L., Ingham, E. S., Leslie, C. A., McGranahan, G. H., Batra, N., Goyal, S., Joseph, J., Jemmis, E. D., Dandekar, A. M., 2011. Mechanism of gallic acid biosynthesis in bacteria (*Escherichia coli*) and walnut (*Juglans regia*). Plant Mol. Biol. 75, 555-565. https://doi.org/ 10.1007/s11103-011-9739-3.

Nandy, M., Ganguli, N. C., 1961. Studies on 5-dehydroshikimic reductase from mung bean seedlings (*Phaseolus aureus*). Arch. Biochem. Biophys. 92, 399-408. https://doi.org/ 10.1016/0003-9861(61)90378-2.

Niggeweg, R., Michael, A. J., Martin, C., 2004. Engineering plants with increased levels of the antioxidant chlorogenic acid. Nat. Biotechnol. 22, 746-754. https://doi.org/ 10.1038/nbt966.

Peek, J., Shi, T., Christendat, D., 2014. Identification of novel polyphenolic inhibitors of shikimate dehydrogenase (AroE). J. Biomol. Screen 19, 1090-1098. https://doi.org/10.1177/1087057114527127.

Rothe, G. M., 1974. Intracellular compartmentation and regulation of two shikimate dehydrogenase isoenzymes in *Pisum sativum*. Z. Pflanzenphysiol. Bd. 74, 152-159. https://doi.org/10.1016/S0044-328X(74)80168-6.

Ryšlavá, H., Doubnerová, V., Müller, K., Baťková, P., Schnablová, R., Liberda, J., Synková, H., Čeřovská, N., 2007. The enzyme kinetics of the NADP-malic enzyme from tobacco leaves. Czech. Chem. Commun. 72, 1420-1434. https://doi.org/1410.1135/cccc20071420.

Singh, S. A., Christendat, D., 2006. Structure of Arabidopsis dehydroquinate dehydratase-shikimate dehydrogenase and implications for metabolic channeling in the shikimate pathway. Biochemistry 45, 7787-7796. https://doi.org/10.1016/S0044-328X(74)80168-6.

Spoustova, P., Hyskova, V., Muller, K., Schnablova, R., Ryslava, H., Cerovska, N., Malbeck, J., Cvikrova, M., Synkova, H., 2015. Tobacco susceptibility to *Potato virus Y*-NTN infection is affected by grafting and endogenous cytokinin content. Plant Sci. 235, 25-36. https://doi.org/ 10.1016/j.plantsci.2015.02.017.

Tahara, K., Nishiguchi, M., Funke, E., Miyazawa, S.-I., Miyama, T., Milkowski, C., 2021. Dehydroquinate dehydratase/shikimate dehydrogenases involved in gallate biosynthesis of the aluminum-tolerant tree species *Eucalyptus camaldulensis*. Planta 253, doi: 10.1007/s00425-020-03516-w. https://doi.org/10.1007/s00425-00020-03516-w.

Tintino, S. R., Oliveira-Tintino, C. D., Campina, F. F., Silva, R. L., Costa Mdo, S., Menezes, I. R., Calixto-Junior, J. T., Siqueira-Junior, J. P., Coutinho, H. D., Leal-Balbino, T. C., Balbino, V. Q., 2016. Evaluation of the tannic acid inhibitory effect against the NorA efflux pump of *Staphylococcus aureus*. Microb. Pathog. 97, 9-13. https://doi.org/ 10.1016/j.micpath.2016.04.003.

Tupec, M., Hyskova, V., Belonoznikova, K., Hranicek, J., Cerveny, V., Ryslava, H., 2017. Characterization of some potential medicinal plants from Central Europe by their antioxidant capacity and the presence of metal elements. Food Biosci. 20, 43-50. https://doi.org/10.1016/j.fbio.2017.08.001.

Tzin, V., Galili, G., 2010. New insights into the shikimate and aromatic amino acids biosynthesis pathways in plants. Mol. Plant 3, 956-972. https://doi.org/ 10.1093/mp/ssq048.

Appendix A. Supplementary Data

Supplementary figure

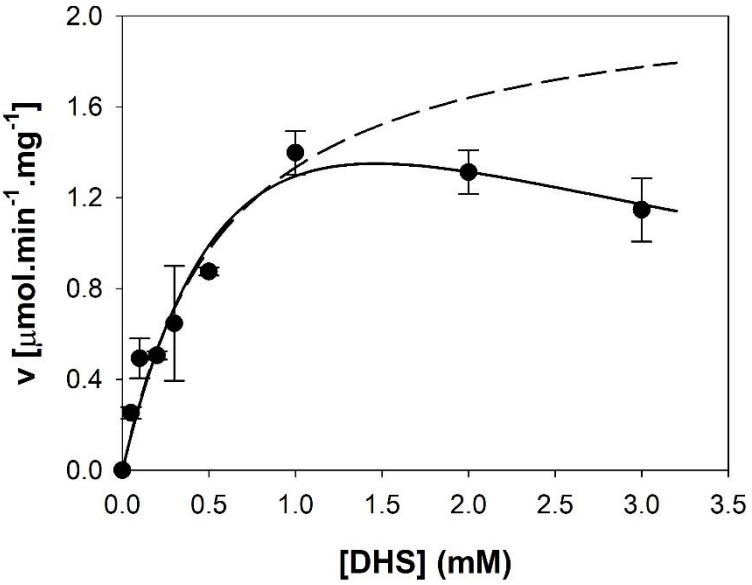

Suppl. Fig. A.1 Inhibition of *P. crispum* SDH by excess of substrate DHS. Dashed line: fit with Michaelis-Menten equation, solid line: fit with Eq. (2) for the inhibition by excess of the substrate.

Supplementary methods

Effect of secondary metabolites on SDH –determination of the reversibility of inhibition
The reversibility of inhibition was tested as follows 30-µl aliquots from the incubation mixture consisting of 200 µl of SDH and 400 µl of 5 mM compound were collected at 0, 1, 5, 10, 15, 20, 30, and 60 mins and assayed, as described above. The blank incubation mixture consisted of 200 µl of SDH, 200 µl of 99 % (v/v) formic acid, and 400 µl of 5 mM inhibitor. The inhibitors primarily dissolved in 96 % ethanol and were diluted to a final 30 % concentration in the reaction mixtures. This percentage of ethanol had no effect on activity in the reference samples.

Derived equations used for the determination of the kinetic mechanism
In order to determine the kinetic parameters of the reaction mechanism, the initial reaction rates were measured for different combinations of the reactants in one or another direction. Under such conditions the reaction-products concentration can be considered as zero and thus the reactions in which they appear as reactants can be dismissed from the mechanism. The reaction scheme of the reaction
$P + Q \rightarrow A + B,$
will therefore adopt the following shape:

$$E + Q \underset{k_{-Q}}{\overset{k_Q}{\rightleftarrows}} EQ \qquad \text{Eq.}(A.1)$$

$$E + P \underset{k_{-P}}{\overset{k_P}{\rightleftarrows}} EP \qquad \text{Eq.}(A.2)$$

$$EQ + P \underset{k_{-1}}{\overset{k_1}{\rightleftarrows}} EPQ \qquad \text{Eq.}(A.3)$$

$$EPQ \xrightarrow{k_B} EA + B \qquad Eq.(A.4)$$

$$EA \xrightarrow{k_A} E + A \qquad Eq.(A.5)$$

In accord with the steady-state approximation we assume the steady state of all the enzyme forms taking place in the mechanism which leads to the following equations:

$$\frac{d[EQ]}{dt} = k_Q[E][Q] - k_{-Q}[EQ] - k_1[EQ][P] + k_{-1}[EPQ] = 0 \qquad Eq.(A.6)$$

$$\frac{d[EP]}{dt} = k_P[E][P] - k_{-P}[EP] = 0 \qquad Eq.(A.7)$$

$$\frac{d[EPQ]}{dt} = k_1[EQ][P] - k_{-1}[EPQ] - k_B[EPQ] = 0 \qquad Eq.(A.8)$$

$$\frac{d[EA]}{dt} = k_B[EPQ] - k_A[EA] = 0 \qquad Eq.(A.9)$$

A similar equation for the last enzyme form, i.e. free enzyme E, is linearly dependent on the previous equation and therefore not used here. In addition, the mass-balance equation

$$[E]_0 = [E] + [EQ] + [EP] + [EPQ] + [EA] \qquad Eq.(A.10)$$

is taken into account – it expresses the fact that all the concentrations of the enzyme forms sum up to the total enzyme concentration present in the reaction mixture.

The reaction rate can be defined as the rate of the conversion of the EPQ complex to a complex EA and the product B (eq. A.4):

$$v = k_B[EPQ]. \qquad Eq.(A.11)$$

(Considering only the initial rates, there are no reverse reaction steps behind the EPQ complex. Therefore, we can equally define the overall reaction rate as a rate of eq. A.5, i.e. $v = k_A[EA]$, obviously obtaining the same result. From the same reason it is not necessary to consider more detailed mechanism of converting the EPQ complex to the final products, e.g. including its transformation to an EAB complex.)

Hence, we express all the concentrations of the enzyme forms as functions of $[EPQ]$. Eq. (A.9) and A.8 give the following relations:

$$[EA] = \frac{k_B}{k_A}[EPQ] \qquad Eq.(A.12)$$

$$[EQ] = \frac{k_{-1} + k_B}{k_1[P]}[EPQ] \qquad Eq.(A.13)$$

Eq. A.7 gives

$$[EP] = \frac{k_P}{k_{-P}}[E][P] \qquad Eq.\ (A.14)$$

and from eq. A.6 we obtain

$$k_Q[E][Q] = \big(k_{-Q} + k_1[P]\big)[EQ] - k_{-1}[EPQ]$$

$$= \big(k_{-Q} + k_1[P]\big)\frac{k_{-1} + k_B}{k_1[P]}[EPQ] - k_{-1}[EPQ] \qquad Eq.(A.15)$$

and thus

$$k_Q k_1[P][Q][E] = \big(k_{-Q} + k_1[P]\big)(k_{-1} + k_B)[EPQ] - k_{-1}k_1[P][EPQ] \qquad Eq.(A.16)$$

$$k_Q k_1[P][Q][E] = \left(k_{-Q}k_{-1} + k_{-Q}k_B + k_B k_1[P]\right)[EPQ] \qquad Eq.(A.17)$$

$$[E] = \frac{\left(k_{-Q}k_{-1} + k_{-Q}k_B + k_B k_1[P]\right)}{k_Q k_1[P][Q]}[EPQ]. \qquad Eq.(A.18)$$

Substituting this expression into eq. A.14 gives

$$[EP] = \frac{k_P}{k_{-P}}\frac{\left(k_{-Q}k_{-1} + k_{-Q}k_B + k_B k_1[P]\right)}{k_Q k_1[Q]}[EPQ]. \qquad Eq.(A.19)$$

Expressions given by eqs. A.12, A.13, A.18, A.19 can be substituted to eq. A.10 which leads to

$$\begin{aligned}[E]_0 &= \left(\frac{k_{-Q}k_{-1} + k_{-Q}k_B + k_B k_1[P]}{k_Q k_1[P][Q]} + \frac{k_{-1} + k_B}{k_1[P]} + \frac{k_P}{k_{-P}}\frac{k_{-Q}k_{-1} + k_{-Q}k_B + k_B k_1[P]}{k_Q k_1[Q]} + 1 \right.\\ &\quad \left. + \frac{k_B}{k_A}\right)[EPQ]\\ &= \frac{1}{[P]}\frac{1}{[Q]}\left(\frac{k_{-Q}}{k_Q}\frac{k_{-1} + k_B}{k_1} + \frac{k_B k_1}{k_Q k_1}[P] + \frac{k_{-1} + k_B}{k_1}[Q] + \frac{k_P}{k_{-P}}\frac{k_{-Q}}{k_Q}\frac{k_{-1} + k_B}{k_1}[P]\right.\\ &\quad \left. + \frac{k_P}{k_{-P}}\frac{k_B k_1}{k_Q k_1}[P]^2 + \frac{k_A + k_B}{k_A}[P][Q]\right)[EPQ]\\ &= \frac{1}{[P]}\frac{1}{[Q]}\left[\frac{k_{-Q}}{k_Q}\frac{k_{-1} + k_B}{k_1} + \frac{k_{-1} + k_B}{k_1}[Q] + \left(\frac{k_P}{k_{-P}}\frac{k_{-Q}}{k_Q}\frac{k_{-1} + k_B}{k_1} + \frac{k_B k_1}{k_Q k_1}\right)[P]\right.\\ &\quad \left. + \frac{k_P}{k_{-P}}\frac{k_B k_1}{k_Q k_1}[P]^2 + \frac{k_A + k_B}{k_A}[P][Q]\right][EPQ] \qquad Eq.(A.20)\end{aligned}$$

From this equation we obtain

$$[EPQ] = \frac{[E]_0[P][Q]}{\frac{k_{-Q}}{k_Q}\frac{k_{-1} + k_B}{k_1} + \frac{k_{-1} + k_B}{k_1}[Q] + \left(\frac{k_P}{k_{-P}}\frac{k_{-Q}}{k_Q}\frac{k_{-1} + k_B}{k_1} + \frac{k_B k_1}{k_Q k_1}\right)[P] + \frac{k_P}{k_{-P}}\frac{k_B k_1}{k_Q k_1}[P]^2 + \frac{k_A + k_B}{k_A}[P][Q]} \qquad Eq.(A.21)$$

and, considering eq. A.11,

$$\begin{aligned}v = k_B[EPQ] &= \frac{k_A k_B}{k_A + k_B}[E]_0[P][Q]\left[\frac{k_A}{k_A + k_B}\frac{k_{-Q}}{k_Q}\frac{k_{-1} + k_B}{k_1} + \frac{k_A}{k_A + k_B}\frac{k_{-1} + k_B}{k_1}[Q]\right.\\ &\quad \left. + \frac{k_A}{k_A + k_B}\left(\frac{k_P}{k_{-P}}\frac{k_{-Q}}{k_Q}\frac{k_{-1} + k_B}{k_1} + \frac{k_B}{k_Q}\right)[P] + \frac{k_A}{k_A + k_B}\frac{k_P}{k_{-P}}\frac{k_B}{k_Q}[P]^2 + [P][Q]\right]^{-1}\\ &= \frac{v_{max}[P][Q]}{K_A + K_{mP}[Q] + K_{mQ}[P] + K_x[P]^2 + [P][Q]} \qquad Eq.(A.22)\end{aligned}$$

The constants in eq. A.22 are defined as follows:

$$v_{max} = \frac{k_A k_B}{k_A + k_B}[E]_0 \qquad Eq.(A.23)$$

$$K_A = \frac{k_A}{k_A + k_B}\frac{k_{-Q}}{k_Q}\frac{k_{-1} + k_B}{k_1} \qquad Eq.(A.24)$$

$$K_{mP} = \frac{k_A}{k_A + k_B}\frac{k_{-1} + k_B}{k_1} \qquad Eq.(A.25)$$

$$K_{mQ} = \frac{k_A}{k_A + k_B}\left(\frac{k_P}{k_{-P}}\frac{k_{-Q}}{k_Q}\frac{k_{-1} + k_B}{k_1} + \frac{k_B}{k_Q}\right) \qquad Eq.(A.26)$$

$$K_x = \frac{k_A}{k_A + k_B}\frac{k_P}{k_{-P}}\frac{k_B}{k_Q} \qquad Eq.(A.27)$$

All the symbols, except for K_x, were chosen in analogy with the conventions used at the ordered two-substrate mechanism. The symbol v_{max}, in the current mechanism, does not have the meaning of the limit maximum reaction rate, since at high concentrations of P inhibition by substrate takes place inevitably. Therefore, it is only a formal symbol resembling the ordered mechanism that adopts the original meaning in case that $K_x \to 0$.

The reciprocal dependence of $\frac{1}{v}$ on $\frac{1}{[P]}$ and $\frac{1}{[Q]}$ then reads

$$\frac{1}{v} = \frac{1}{v_{max}}\left(K_A\frac{1}{[P]}\frac{1}{[Q]} + K_{mP}\frac{1}{[P]} + K_{mQ}\frac{1}{[Q]} + K_x\frac{[P]}{[Q]} + 1\right) \qquad Eq.(A.28)$$

The following relations can be found among the constants in eq. A.28:

$$K_A = \frac{k_{-Q}}{k_Q}K_{mP} \qquad Eq.(A.29)$$

$$K_{mQ} = \frac{k_P}{k_{-P}}K_A + \frac{k_{-P}}{k_P}K_x \qquad Eq.(A.30)$$

As K_{mP} is independent of k_Q and k_{-Q} and K_A is independent of k_P and k_{-P}, the constants K_A, K_{mP}, K_{mQ}, K_x are independent in the sense that they may adopt any combination of values without being determined by one another. Thus, when determining them from the experimental data we need not work with the individual rate constants but we can only take these cumulative constants into account.

Eqs. A.22 and A.28 can be analogously applied at the initial-velocity experiments with the reverse reaction, i.e.

$A + B \to P + Q$.

In this case we substitute $Q \to A$ and $P \to B$ and obtain

$$v = \frac{v_{max}[B][A]}{K'_A + K_{mB}[A] + K_{mA}[B] + K'_x[B]^2 + [B][A]} \qquad Eq.(A.31)$$

and

$$\frac{1}{v} = \frac{1}{v_{max}}\left(K'_A\frac{1}{[B]}\frac{1}{[A]} + K_{mP}\frac{1}{[B]} + K_{mQ}\frac{1}{[A]} + K'_x\frac{[B]}{[A]} + 1\right). \qquad Eq.(A.32)$$